

The Effect of the Signaling Scheme on the Robustness of Pattern Formation in Development

Hye-Won Kang, Likun Zheng and Hans G. Othmer*

School of Mathematics
University of Minnesota
Minneapolis, MN 55455

Abstract

Pattern formation in development is a complex process that involves spatially-distributed signals called morphogens that influence gene expression and thus the phenotypic identity of cells. Usually different cell types are spatially segregated, and the boundary between them may be determined by a threshold value of some state variable. The question arises as to how sensitive the location of such a boundary is to variations in properties, such as parameter values, that characterize the system. Here we analyze both deterministic and stochastic reaction-diffusion models of pattern formation with a view toward understanding how the signaling scheme used for patterning affects the variability of boundary determination between cell types in a developing tissue.

1 Introduction

1.1 Morphogenetic fields and positional information

The emergence of new cellular phenotypes during the development of organisms involves both the selection of a particular developmental pathway via transcription of one or more genes, and differentiation, which involves protein production and other downstream steps. Both processes are usually tightly coupled, and hereafter we simply speak of differentiation. Although differentiation is a cell-level process and can occur in isolated cells, our focus is on differentiation in a tissue containing many cells, and in particular, on how reliably the spatial location of the boundary between distinct cell types can be specified under various signaling schemes. Such spatially-varying differentiation, or pattern formation, requires the appropriate spatial pattern of a transcription factor or other cellular state variable, and this pre-existing pattern or pre-pattern may be maternally inherited, it may stem from an earlier spatially-controlled pattern of gene expression, or it may arise spontaneously within the tissue. Thus pattern formation is a hierarchical process in which successive steps build on pattern formation in previous steps.

The local distribution of extracellular molecular species, mechanical stresses and other factors defines the morphogenetic landscape from which cells extract information, and frequently alter by release of components into the extracellular space. In the simplest case diffusible molecules called morphogens, a term coined by Turing [1], affect the internal state in a concentration-dependent manner. More precisely,

*All authors contributed equally to this paper.

1 morphogens are defined as secreted signaling molecules that (i) are produced in a tissue, frequently in a
2 restricted region, (ii) are transported by diffusion [2], active transport, relay mechanisms, or other means
3 within the tissue [3], (iii) are detected by specific receptors or bind to regulatory regions of DNA, and
4 (iv) initiate an intracellular signal transduction cascade that initiates or terminates the expression of
5 target genes in a concentration-dependent manner. The concept of a morphogenetic landscape, usually
6 described as a developmental field similar to the classical fields in physics, played a role throughout
7 the early history of theoretical work in pattern formation [4, 5]. When morphogens are the carriers of
8 the extracellular state, the morphogenetic landscape usually varies smoothly in space, but the response
9 to an established pre-pattern may require conversion of a smoothly-varying extracellular signal into a
10 step-like response via some downstream mechanism.

11 The establishment of pattern from spatial homogeneity is called Turing’s problem [1], which is to
12 specify mechanisms under which an aggregate of cells, all initially in similar states, undergoes a well-
13 defined spatial pattern of differentiation leading to a nonuniform distribution of cell types. In Turing’s
14 model, two or more morphogens react within each cell and diffuse between cells. All cells are assumed to
15 be identical initially, and under appropriate boundary conditions, the reaction-diffusion equations that
16 describe the model have a solution that is spatially-uniform. What Turing showed is that this uniform
17 state can be unstable to some non-uniform disturbances if the kinetic interactions and the diffusion
18 constants are chosen appropriately. Such instabilities, which Turing called symmetry-breaking, can lead
19 to a steady or a time-periodic nonuniform distribution of morphogens. The unstable wavelengths are
20 fixed by the kinetic coefficients and the diffusivities, and therefore each unstable system has an intrinsic
21 chemical wavelength. Thus identical systems will give rise to an identical distribution of morphogens
22 and, via an appropriate interpretation mechanism, to an identical pattern of cell differentiation. Turing
23 himself suggested that the model could account for the regular spacing of tentacles on Hydra and that
24 it might be applicable to phyllotaxis. Many generalizations and applications of the model have been
25 proposed [6, 7, 8, 9].

26 Turing’s original model may be well-suited for explaining mosaic development, in which removal of
27 a part of a developing embryo at one stage results in the absence of that part in later stages, but it is
28 less successful in predicting the degree of resilience or robustness of patterning in response to changes in
29 the size of an organism, the strength of inputs, or the values of the many parameters involved in signal
30 transduction and gene control networks. Some degree of regulation for simple patterns can be achieved
31 using simple reaction-diffusion models, as will be shown later, but more complex schemes are often
32 needed. One approach is to postulate that the kinetic and transport coefficients are space dependent
33 to reflect the past history of development. This is certainly in the direction of greater biological reality
34 because, as Turing himself observed, ‘Most of an organism, most of the time, is developing from one
35 pattern into another, rather than from homogeneity into a pattern’ [1]. What remains in doubt is
36 whether the mechanism in its original form, which generates pattern via an instability of a uniform state,
37 is applicable to biological systems. Whatever the ultimate status of Turing’s theory as a mechanism
38 of biological pattern formation may be, it has both stimulated a tremendous amount of research and
39 strongly influenced how spatial pattern formation in biology is understood by emphasizing the important
40 role of the interaction between reaction and diffusion.

41 Another widely-studied class of morphogen-based models are those in which morphogen production
42 is spatially-localized. These are often called positional information (PI) models, in that a cell must

1 ‘know’ its position relative to other cells in order to adopt the correct developmental pathway [10],
 2 but they could also be called pre-pattern models, since the next stage of patterning is predicated on
 3 gene expression or morphogen production in a previous stage. In practice, in both Turing’s model and
 4 most PI models the system is usually regarded as an initially spatially-homogeneous medium, transport
 5 is described by Fick’s law, and cell-cell-communication is indirect via secretion into the extracellular
 6 space, followed by re-uptake by a variety of mechanisms. However, previous rounds of patterning may
 7 establish spatial variations in expression of various signaling molecules, as in dorsal-ventral patterning
 8 in the *Drosophila* embryo [11], and there are several other modes of cell-cell communication that may
 9 play a role [12]. Detailed models of endo- and exocytosis have not been included in this context, for this
 10 is a formidable task, as the example of the *Drosophila* wing disc shown in Figure 1(left) suggests. The
 11 signaling networks in the disc add another level of complexity to the geometric complexity, as shown
 12 in Figure 1(right). The principle morphogens are hedgehog (Hh), decapentaplegic (Dpp), and wingless
 13 (Wg), and one sees that each of the primary pathways has feedback loops and cross-interactions with
 14 other pathways. In particular, there is a negative feedback loop in each of the three: through Ptc –
 15 Smo – CiA – Ptc in the Hh pathway, through Tkv– pMad – Brk – Omb – Tkv in the Dpp pathway,
 16 and through Dfz – Dsh – Arm – Dfz in the Wg pathway. The complexity in the interactions of the
 17 different transport and signaling processes is frequently hidden when interpreting experimental data,
 18 because the spread of morphogens is analyzed using a simple reaction-diffusion system [13]. However
 19 it is usually difficult to relate the individual steps in what may be a very complex process to such a
 20 high-level description, and homogenization of the disc so as to preserve the relevant biochemical and
 21 mechanical interactions at the cell level is beyond reach at present.

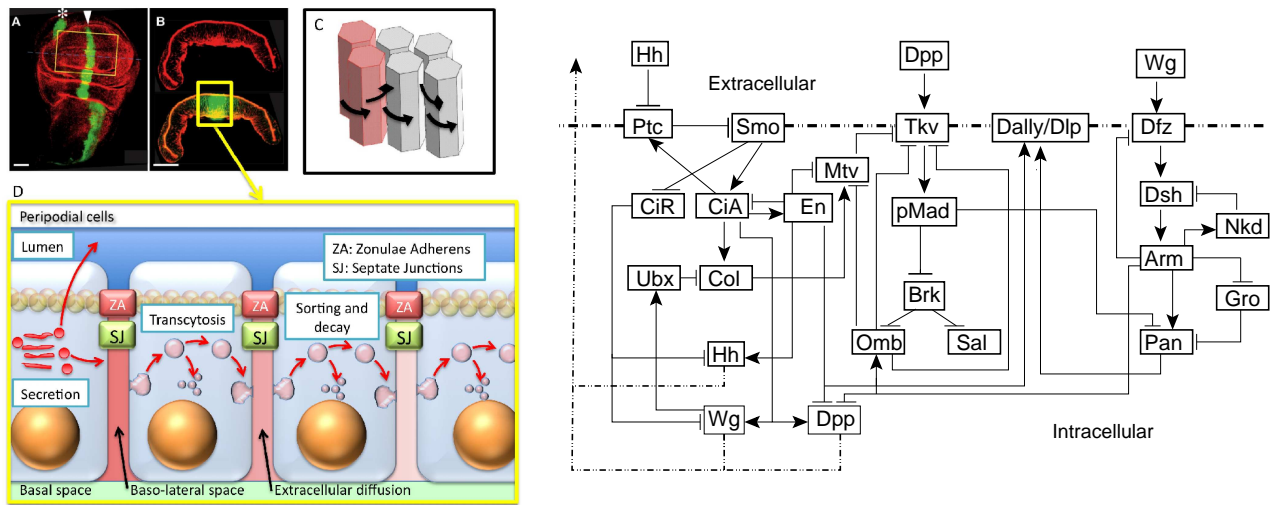


Figure 1: (Left) Patterning of epithelial cells in the *Drosophila* wing imaginal disc by Dpp. (A) Top view showing the pouch and (B) a slice along the midline in (A) showing the geometry of the columnar cells. (C-D) Patterning involves several reaction and transport processes that affect the Dpp distribution, including diffusion around columnar cells (C) or transcytosis through columnar cells (D). (From [12], with permission.) (Right) Primary components in the signaling network for wing disc patterning. Ptc: patched, Smo: smoothed, CiA(R): cubitus interruptus activator (repressor), Ubx: ultrabithorax, Col: collier, Dfz: *Drosophila*frizzled, Dsh: disheveled, Nkd: naked, Gro: groucho, Pan: pangolin.

22 The most widely-studied type of pre-pattern for morphogen signaling involves specialized spatial
 23 regions that are either maternally-specified or determined in previous patterning steps, and that produce

1 morphogen and release it into the extracellular space. The morphogen is then either actively or passively
 2 transported throughout the tissue, to be interpreted locally
 3 by cells according to their position in the morphogenetic land-
 4 scape. We call the interpretation of the morphogen distribu-
 5 tion the *response*. Here we treat it as a scalar variable that
 6 depends on both morphogen levels and other factors that turn
 7 specified genes on or off, and this dependence is encoded in the
 8 *response functional*. We call the combination of one or more
 9 specified morphogen sources and a downstream interpretation
 10 mechanism a *signaling scheme*. This is a generalization of
 11 the motif concept used in studying networks [15], in that the
 12 same motif may be used either in combination with different
 13 morphogen sources or different response functionals. Our ob-
 14 jective is to analyze how different signaling schemes affect the
 15 sensitivity, the precise measure of which is defined later, of
 16 the spatial location of a specified response level to paramet-
 17 ric changes. An example of a signaling scheme that arises in
 18 the early development of vertebrate limbs is shown in Figure
 19 2. This example is more complicated than those we analyze
 20 later, but it illustrates the interplay of the spatial location of
 21 morphogen sources and the network of the downstream inter-
 22 actions, a theme that will recur throughout. Some of the effects of morphogen interactions in limb bud
 23 development have been analyzed [16], but a much more systematic approach along the lines developed
 24 later is needed. A more detailed discussion of related issues in pattern formation appears in [12].

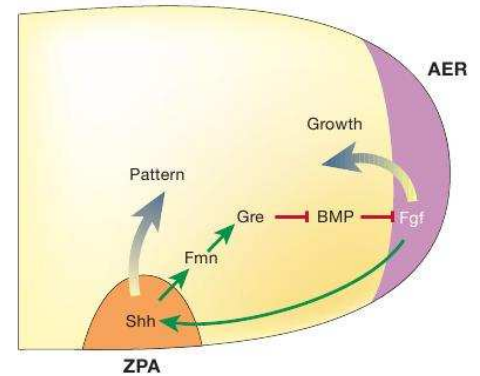


Figure 2: The signaling scheme used in develop-
 ment of the vertebrate limb. A morphogen pro-
 duced in the zone of polarizing activity (ZPA) is
 part of a feedback loop that controls production
 of growth factors in the apical ectodermal ridge
 (AER), which in turn affects production of the
 morphogen. The intermediate steps, which are
 not shown in detail, involve formin, gremlin, bone
 morphogenetic protein, and fibroblast growth
 factor. From [14] (with permission).

25 1.2 The dynamic *vs.* static interpretation of morphogen levels

26 The first species known to serve as a morphogen in the foregoing sense is Bicoid, a protein that is
 27 produced from maternally-inherited mRNA embedded in the anterior 20% of the plasma membrane of
 28 the embryo [17]. Bicoid is a transcription factor that initiates a hierarchy of sequential gene expression
 29 that involves the gap genes, the pair-rule genes and ultimately the segment polarity genes [12]. In the
 30 early stages the embryo is a syncytium with nuclei spread throughout the cytoplasm, but later the nuclei
 31 are embedded in the surrounding membrane. Bicoid production in the anterior portion of the embryo
 32 gives rise to a spatial distribution of the protein [18], and since the earliest gap gene expression occurs
 33 about 1.5 hours after egg deposition, the question arises as to whether the Bicoid gradient is essentially
 34 at steady state at this time. Others have addressed this issue [19, 20, 21], but some important aspects
 35 deserve re-examination. In the remainder of this section we analyze how reaction and diffusion interact
 36 to determine the time scale for relaxation to the steady state distribution, and we show how to track
 37 the propagation of a chosen concentration level into the domain. In regard to the latter, we show that
 38 depending on the signaling scheme, the position of a threshold level of morphogen may first overshoot
 39 its location in the steady state and then retreat. In regard to the former we show that the relaxation

Table 1: Symbols and their definitions

Symbol	Meaning
c	Morphogen concentration
t	Time variable
x	Space variable
k	Morphogen decay rate
K	Reference concentration used for nondimensionalization
L	Length of the domain
\mathcal{D}	Morphogen diffusion constant
j	Morphogen input flux
$u = c/K$	Dimensionless morphogen concentration
$\xi = x/L$	Dimensionless space variable
$\tau = kt$	Dimensionless time variable
$\delta^2 = \mathcal{D}/(kL^2)$	Dimensionless diffusion constant
$J = jL/(K\mathcal{D})$	Dimensionless input flux
T_1	The time-scale for relaxation to the steady-state
\mathcal{R}	The symbol for the response functional that determines the response to a morphogen gradient. Its definition depends on the signaling scheme.
∇	The gradient operator
Δ	The Laplace operator, $= \nabla \cdot \nabla$
V_n	The normal velocity of a level set
\mathbf{n}_c	The unit normal to a level set

1 time to the steady state is given by ¹

$$2 \quad T_1 \equiv \frac{1}{\frac{\mathcal{D}\pi^2}{L^2} + k}. \quad (1.1)$$

3 From this one sees that either diffusion or morphogen decay can dominate the relaxation process, and
4 their effect is additive. Furthermore, the contribution of diffusion decreases with a decrease in \mathcal{D} or an
5 increase in L , while that of protein decay affects the time similarly. Estimates of the half-life of Bicoid
6 range from ~ 8 mins [22] to less than ~ 30 mins [21], and we use 20 mins as an intermediate estimate,
7 and thus $k = 0.05 \text{ min}^{-1}$. Estimates of the diffusion coefficient range upward from $0.3 \mu\text{m}^2/\text{sec}$ [21],
8 and thus for the lowest \mathcal{D} and an embryo length of $L = 500 \mu\text{m}$, the relaxation time of the slowest
9 decaying mode is ~ 20 mins, and is determined almost solely by the degradation rate. If the foregoing
10 estimate of k is accurate, then there are several half-lives of the slowest mode in the approximately 1.5
11 hour period from egg-laying to appearance of gap gene expression in cycle 10 [23], and one can assume
12 that the Bicoid gradient has stabilized at this time.

The simplest model for describing the spatial distribution of Bicoid protein is based on a one-dimensional spatial domain, with protein synthesis localized at the anterior pole, transport by diffusion throughout the syncytium, and a uniform protein decay rate. While this model is over-simplified and

¹The definition of symbols used here and later are given in Table 1.

the system is more complex in reality, for instance in respect to the localization of protein synthesis [22, 17], it serves as a model that illustrates the underlying concepts. The governing equations for the time-dependent morphogen concentration c , assuming that transcription, and hence the influx of Bicoid, is turned on at $t = 0$, describe the evolution of the concentration of the morphogen due to the effects of reaction and diffusion in the interior of the domain, combined with conditions that describe the influx at the anterior pole and the fact that there is no loss of morphogen at the posterior pole.

$$\begin{aligned}
\frac{\partial c}{\partial t} &= \mathcal{D} \frac{\partial^2 c}{\partial x^2} - kc & x \in (0, L) \\
-\mathcal{D} \frac{\partial c}{\partial x} &= j & x = 0 \\
\frac{\partial c}{\partial x} &= 0 & x = L \\
c(x, 0) &= 0. & x \in (0, L)
\end{aligned} \tag{1.2}$$

1 It is not difficult to relax the assumption that the mRNA is localized at the anterior pole by adding a
2 space-dependent source to the right-hand side of (1.2) and setting $j = 0$, and this has been done in [17].

We convert these equations to dimensionless form by defining $\xi = x/L$, $\tau = kt$, $\delta^2 = \mathcal{D}/(kL^2)$, $J = jL/(K\mathcal{D})$ and $u = c/K$, where K is specified later. Then the equations become

$$\begin{aligned}
\frac{\partial u}{\partial \tau} &= \delta^2 \frac{\partial^2 u}{\partial \xi^2} - u & \xi \in (0, 1) \\
-\frac{\partial u}{\partial \xi} &= J & \xi = 0 \\
\frac{\partial u}{\partial \xi} &= 0 & \xi = 1 \\
u(\xi, 0) &= 0. & \xi \in (0, 1)
\end{aligned} \tag{1.3}$$

The steady-state solution satisfies

$$\begin{aligned}
\delta^2 \frac{d^2 u^s}{d\xi^2} &= u^s & \xi \in (0, 1) \\
-\frac{du^s}{d\xi} &= J & \xi = 0 \\
\frac{du^s}{d\xi} &= 0 & \xi = 1,
\end{aligned} \tag{1.4}$$

3 The solution of this is

$$4 \quad u^s(\xi) = J\delta \left[\frac{e^{-\xi/\delta} + e^{(\xi-2)/\delta}}{1 - e^{-2/\delta}} \right] \equiv J\delta\phi(\xi) = \frac{j}{K\sqrt{k\mathcal{D}}}\phi(\xi). \tag{1.5}$$

5 From this solution one sees that the spatial decay of the morphogen gradient is governed by $\delta =$
6 $\sqrt{\mathcal{D}/(kL^2)} = \sqrt{T_k/T_d}$, which involves the ratio of a kinetic time scale $T_k \equiv k^{-1}$ to a diffusion time scale
7 $T_d \equiv L^2/\mathcal{D}$. Thus reducing the kinetic scale by reducing the half-life of the morphogen, or increasing
8 the diffusion time scale by decreasing the diffusion constant, leads to sharper, more rapidly-decreasing
9 spatial profiles. While it is sometimes assumed that this combination also controls the approach to the
10 steady state, we see from (1.1) that this is not the case. It should also be noted that the second term in

1 both the numerator and denominator of (1.5) arises from the finite length of the domain, and can only
 2 be neglected if $\delta \ll 1$.

3 To derive the expression in (1.1) for the time-scale for approach to the steady state, we observe that
 4 the difference $w \equiv u - u^s$, which captures the transient component of the solution, satisfies (1.3) with
 5 $J = 0$ and $w(\xi, 0) = -u^s(\xi)$. The solution of the resulting system is

$$6 \quad w(\xi, \tau) = \sum_{n=1}^{\infty} a_n e^{-\lambda_n \tau} \cos n\pi\xi, \quad (1.6)$$

7 wherein the constants a_n are determined by the steady-state solution. The exponential decay rates λ_n
 8 are given by

$$9 \quad \lambda_n = \delta^2 (n\pi)^2 + 1 \quad n = 1, 2, \dots \quad (1.7)$$

10 and the smallest of these, λ_1 , defines the relaxation time of the slowest decaying mode $\cos(\pi\xi)$ in
 11 the transient solution. The reciprocal of this is a dimensionless relaxation time, and converting it to
 12 dimensional form leads to (1.1). As stated earlier, one can conclude that there is adequate time for
 13 establishment of the Bicoid gradient in *Drosophila*, even if the half-life of Bicoid is 30 mins.

14 There is also adequate time for stabilization of the morphogen distribution in other systems. For
 15 example in the *Drosophila* wing disc the patterning occurs over several days, but the profile of the dom-
 16 inant morphogen Dpp is established in about eight hours [24]. However, in some systems, particularly
 17 those involving feedback in the early steps in signal transduction, the pattern of gene expression evolves
 18 significantly in time. In dorsal-ventral patterning of the *Drosophila* embryo, the downstream factor
 19 pMad is first expressed in a broadly-distributed, low-level pattern, and later sharpens dramatically to
 20 localize patterning of the amnioserosa [25], and this has been explained with a model based on a positive
 21 feedback loop that controls production of a protein that acts as a co-receptor [26, 11].

22 Of course this does not mean that gene expression does not begin until the spatial distribution of
 23 the morphogen stabilizes. When the local morphogen concentration is time-varying, the downstream
 24 response may be determined by the instantaneous or time-delayed morphogen concentration, there may
 25 be no response until the absolute or integrated signal exceeds a certain level, or the response may adapt
 26 in time and thus require a minimal rate of change of the signal [27]. In many cases the morphogen
 27 production is switched on at time zero, and it is of interest to determine how fast the concentration
 28 of morphogen rises at any given spatial location. In the context of *Drosophila* AP patterning, gene
 29 expression probably begins as soon as a critical concentration is exceeded, which implies that one
 30 should observe a Bicoid-initiated wave of Hunchback expression that propagates down the AP axis. We
 31 analyze this for general systems here by computing the speed of propagation of surfaces of constant
 32 concentration (level sets) in reaction-diffusion systems. We do this for any spatial dimension, and thus
 33 the level sets can be curved and their curvature will affect the speed of propagation.

34 First consider a slight generalization of (1.2) written as

$$35 \quad \frac{\partial c}{\partial t} = \mathcal{D}\Delta c + f(c) \quad (1.8)$$

36 and suppose that a level set $c \equiv c_0 = \text{constant}$ is defined by specifying the position vector $\mathbf{r}(t)$ of any
 37 point on the surface. Then an observer moving with that surface sees no change, which means that the
 38 Lagrangian derivative of c evaluated on that surface vanishes, *i.e.*,

$$\left. \frac{dc}{dt} \right|_{c=c_0} = 0 = \frac{\partial c}{\partial t} + \nabla c \cdot \frac{d\mathbf{r}}{dt} = \frac{\partial c}{\partial t} - V_n |\nabla c|.$$

Here the normal vector to the surface and the speed in the normal direction are defined as

$$\mathbf{n}_c \equiv -\frac{\nabla c}{|\nabla c|} \quad \text{and} \quad V_n \equiv \mathbf{n}_c \cdot \frac{d\mathbf{r}}{dt},$$

- 1 and all terms are evaluated at $c = c_0$. By definition the normal is directed toward decreasing c levels.
 2 Therefore, if $|\nabla c| \neq 0$, then

$$V_n = \left. \frac{c_t}{|\nabla c|} \right|_{c=c_0} = \left. \frac{\mathcal{D}\Delta c + f(c)}{|\nabla c|} \right|_{c=c_0} \equiv \left. \frac{F(c, \Delta c)}{|\nabla c|} \right|_{c=c_0}. \quad (1.9)$$

4 Obviously $V_n > 0$ whenever c_t is positive, and either or both V_n and $|\nabla c|$ vanish on the set where F
 5 vanishes, *i.e.*, where c has reached a steady-state. Furthermore, one sees that the speed of propagation
 6 increases with the magnitude of c_t and decreases with the steepness of the gradient. Thus level sets in
 7 a shallow gradient propagate faster than those in a steep gradient, and the most striking example of
 8 this is the infinite speed of propagation of the zero level set in a pure diffusion process. For a scalar
 9 equation the velocity is of one sign during the approach to a steady state, but this need not be true
 10 in systems, as discussed below. The asymptotic speed of traveling waves of permanent form on infinite
 11 domains is well-understood [28], but the profiles of interest here are not of constant shape.

12 In general the response will be more complex – for example gene expression may be a nonlinear
 13 function of the morphogen level, or it may involve both positive and negative control. We discuss an
 14 extension of the foregoing to two species, but it can easily be done in general. Suppose that the two
 15 morphogens (c_1, c_2) evolve according to

$$\begin{aligned} \frac{\partial c_1}{\partial t} &= \mathcal{D}_1 \Delta c_1 + f(c_1, c_2) \\ \frac{\partial c_2}{\partial t} &= \mathcal{D}_2 \Delta c_2 + g(c_1, c_2), \end{aligned} \quad (1.10)$$

and suppose that the response is given by $\mathcal{R}(c_1, c_2)$. Further suppose that the threshold response
 corresponds to the level set $\mathcal{R} = \mathcal{R}^* = \text{constant}$. As before, this surface moves according to

$$\left. \frac{d\mathcal{R}}{dt} \right|_{\mathcal{R}=\mathcal{R}^*} = 0 = \frac{\partial \mathcal{R}}{\partial t} + \nabla \mathcal{R} \cdot \frac{d\mathbf{r}}{dt} = \frac{\partial \mathcal{R}}{\partial t} - V_{\mathcal{R}} |\nabla \mathcal{R}|$$

If \mathcal{R} depends on both species then

$$\frac{\partial \mathcal{R}}{\partial t} = \frac{\partial \mathcal{R}}{\partial c_1} \frac{\partial c_1}{\partial t} + \frac{\partial \mathcal{R}}{\partial c_2} \frac{\partial c_2}{\partial t} \quad \text{and} \quad |\nabla \mathcal{R}| = \left| \frac{\partial \mathcal{R}}{\partial c_1} \nabla c_1 + \frac{\partial \mathcal{R}}{\partial c_2} \nabla c_2 \right|$$

- 17 and if $\nabla \mathcal{R} \neq 0$ then

$$V_{\mathcal{R}} = \frac{\frac{\partial \mathcal{R}}{\partial c_1} (\mathcal{D}_1 \Delta c_1 + f(c_1, c_2)) + \frac{\partial \mathcal{R}}{\partial c_2} (\mathcal{D}_2 \Delta c_2 + g(c_1, c_2))}{\left| \frac{\partial \mathcal{R}}{\partial c_1} \nabla c_1 + \frac{\partial \mathcal{R}}{\partial c_2} \nabla c_2 \right|}. \quad (1.11)$$

1 From this one sees that it is easy to construct response functionals for which the threshold level set
 2 overshoots its steady state position. Suppose for instance that the spatial domain is one-dimensional,
 3 that $f(c_1, c_2) = -c_1$, $g(c_1, c_2) = -\kappa c_2$, and that ²

$$4 \quad \mathcal{R} = \frac{c_1^m}{1 + c_1^m} \frac{1}{1 + c_2^n}. \quad (1.12)$$

5 Thus c_1 is an activator of the response, and we assume that there is an input flux of c_1 at $x = 0$, while
 6 c_2 acts as an inhibitor and is input at $x = L$. If both inputs are switched on at $t = 0$, and if c_1 relaxes
 7 to its steady state distribution much faster than c_2 does, the rapid establishment of the c_1 profile will
 8 initiate a response in some portion of the domain, but as c_2 gradually increases the threshold level set
 9 movement will reverse and move toward $x = 0$. One can see this most easily by supposing that c_1
 10 reaches steady-state instantaneously. Examples in which there is overshoot are known from systems
 11 in which there is negative feedback via morphogen-stimulated production of a receptor [29, 30]. Other
 12 signaling schemes are possible – *e. g.* , it may also happen that the response involves two activators
 13 produced at opposite ends of the domain, and numerical examples of both activator/inhibitor and dual
 14 activator systems are given later.

15 The response in (1.12) may apply to AP patterning in *Drosophila*, in which we identify the mor-
 16 phogens as Bicoid and Nanos, and the response as Hunchback expression. A similar analysis can be
 17 applied to downstream steps in the gene expression hierarchy in AP patterning, and it is known for
 18 instance that the spatial domains of gap gene expression shift as development proceeds [31]. This system
 19 and others will require other forms of the response functional, and these may have multiple components,
 20 such as $\mathcal{R}_1 \geq \mathcal{R}_1^*$ and $\mathcal{R}_2 \geq \mathcal{R}_2^*$, but the foregoing approach applies in general.

21 1.3 Resilience, robustness and reliability in patterning

22 The overall process of development, including pattern formation, differentiation, growth, and the other
 23 developmental processes, can usually tolerate a certain level of disturbances encountered during de-
 24 velopment and yet produce a normal adult, and we say that such systems regulate. There are many
 25 examples of this, particularly at early stages of development. For instance, each of the cells that results
 26 from the first cleavage in amphibian eggs can, when separated from the other, develop into a normal,
 27 albeit smaller, adult. Certainly this type of regulation requires some form of intercellular communica-
 28 tion and some kind of feedback mechanism whereby removal of part of an organism is sensed by the
 29 remainder, and development is redirected to compensate for the part removed. Here we focus on less
 30 drastic perturbations, and begin by defining some terminology.

31 Robustness, resilience and reliability all capture, to varying degrees, the idea that systems can
 32 develop ‘normally’ under certain types of perturbations. In computer science robustness refers to the
 33 ability of a program to cope with errors in inputs or calculations during execution, and this best describes
 34 the notion that systems can regulate in the sense used previously. Consider a dynamical system of the
 35 form

$$36 \quad \frac{du}{dt} = F(u, \Phi, S(t)) \quad u(0) = u_0 \quad (1.13)$$

37 where u is the state, Φ is a set of parameters, and $S(t)$ is an input. This form is sufficiently general to
 38 encompass the reaction diffusion equations described earlier when u is an element of a suitable Banach

²Here we use the freedom to scale c_1 and c_2 so that the half-maximal values of both are 1.

1 space, and (1.13) is viewed as an evolution equation in that space, but the reader can, without loss of
2 understanding, regard (1.13) as an evolution equation for a finite number of state variables.

3 We can identify at least three classes of perturbations that lead to three types of robustness.

- 4 1. Robustness with respect to changes in model parameters, constant inputs, and so on. One
5 biologically-important example in this class is robustness with respect to changes in the size
6 of the system. A general class of reaction-diffusion systems that show perfect scale-invariance
7 is known [32], and a detailed study of scale-invariance in various patterning mechanisms will be
8 reported elsewhere [33]. This type of robustness can be measured by a suitably-defined sensitivity
9 of the response, examples of which are given later.
- 10 2. Robustness with respect to transient changes in the input $S(t)$. By this we mean that changes
11 in time-dependent external inputs only evoke a transient response, but constant offsets in the
12 input are ignored *in the long run*. Such systems nullify changes in a specified class of inputs
13 by generating the inputs internally and employing suitable feedback to nullify them [34]. In
14 particular, this includes the capability of systems to respond only to transient changes in inputs,
15 and to ignore time-independent inputs.
- 16 3. Robustness with respect to changes in the structure of the equation itself. Systems that are robust
17 in this sense can withstand the inclusion of a new component in a signal transduction pathway
18 without significantly altering the input-output behavior of the system. For small changes in the
19 equation this is described by the mathematical concept of coarseness or structural stability – a
20 vectorfield is structurally stable if its associated flow is orbit equivalent to the flow generated by
21 any vectorfield in a sufficiently small neighborhood in a suitable topology [35]. A global criterion
22 for structural stability is known for linear vector fields in finite dimensions, but only local results
23 are known for nonlinear finite-dimensional systems, and therefore cannot be used for large changes.

24 Several general strategies for reducing sensitivity to perturbations include (i) operation at saturation,
25 which implies that changes in input have no effect, (ii) employment of suitable feedback mechanisms
26 to compensate for changes in inputs, (iii) employment of a hierarchical system, such as that which
27 terminates in the segment polarity genes in *Drosophila*.

28 In the remainder of this paper we focus on the robustness of the location of boundaries between
29 different emerging cell types in a developing tissue under perturbations in boundary inputs and param-
30 eters. As we have already seen, if the boundary is set by a prescribed threshold value of a response
31 functional, then in general it moves during establishment of the morphogen profiles. In the following
32 section we analyze deterministic systems, and in the penultimate section we analyze stochastic systems.
33 In both cases the primary focus is on a static or stationary-in-time interpretation of the response –
34 the dynamic case will be treated elsewhere. We identify a number of distinct types of spatial signaling
35 schemes and analyze the robustness of boundary placement under these distinct schemes.

36 **2 The robustness of boundary placement in deterministic models**

37 **2.1 The French flag problem**

38 In the simplest version of a PI or pre-pattern model, either specialized source and sink cells located at
39 the boundary of the developmental field maintain the concentration of the morphogen at fixed levels, or

1 they produce or destroy the morphogen at a fixed rate. If there is no degradation of morphogen in the
 2 first case, then given fixed thresholds between different cell types, a 1D system can be proportioned into
 3 any number of cell types in a perfectly scale-invariant way. However this scheme is clearly not robust
 4 as it stands, since the flux between source and sink in a 1D system of length L scales as $1/L$, and thus
 5 the morphogen-producing or consuming cells at the boundary must adjust production to adjust for the
 6 size of the system.

7 For the second scheme we consider the simple signaling scheme analyzed earlier, in which the flux
 8 at the boundary, rather than the concentration, is fixed. The steady-state solution given by (1.5) is
 9 characterized by the dimensionless parameter δ that involves the ratio of a kinetic time scale $T_k \equiv k^{-1}$
 10 to a diffusion time scale $T_d \equiv L^2/\mathcal{D}$, and the dimensionless parameter $J\delta$, which we write as

$$11 \quad J\delta = \frac{L}{\sqrt{k\mathcal{D}}} / \left(\frac{j}{KL} \right)^{-1} \equiv \frac{T_{rd}}{T_i}. \quad (2.1)$$

12 This is the ratio of a time scale T_{rd} defined by reaction and transport within the domain, to the
 13 time scale T_i defined by the scaled input KL/j . The parameter δ enters in the shape function ϕ via
 14 the exponential terms and determines how rapidly the morphogen concentration decays in space: if
 15 $T_k \ll T_d$ then $\delta \ll 1$ and the solution decays rapidly from its value at the source. It is clear that for a
 16 fixed input flux j both the amplitude and the shape of the morphogen distribution depend on L , and thus
 17 this simple scheme does not suffice when significant variations in length occur in the developing system.
 18 Perfect shape-invariance could be achieved by modulating \mathcal{D} or k appropriately [32], but robustness
 19 with respect to the input flux requires a more sophisticated scheme since it requires that the ratio in
 20 (2.1) remains constant. More complex patterning driven by pre-patterns can result when there are
 21 several specialized boundary regions, an example of which arises in vertebrate limb development, where
 22 species produced in specialized regions called the ZPA and the AER interact to direct outgrowth and
 23 patterning [36, 16]. Several simple schemes that illustrate some of the effects of multiple inputs are
 24 analyzed later.

25 **2.2 Sensitivity of thresholds in a static interpretation**

26 As stated earlier, our focus in the remainder of the paper is on the robustness of determination of the
 27 boundary between cell types in a developing tissue, and in the remainder of this section we focus on
 28 deterministic models. We first develop a general method for computing one measure of the sensitivity
 29 of the location of a threshold to parametric changes. The measure we adopt is simply the derivative of
 30 the threshold location to a chosen parameter, but since the governing equations are typically nonlinear,
 31 this must be done numerically. A number of specific examples are analyzed in detail in the following
 32 subsections.

33 Suppose that the equations for the local dynamics – binding reactions, enzyme-catalyzed steps, etc.
 34 – are written as the system

$$35 \quad \frac{du}{d\tau} = F(u, \Phi), \quad (2.2)$$

36 where now $u \in \mathbb{R}^n$ represents the dimensionless concentrations and other state variables, while Φ
 37 represents parameters and inputs that we treat as constants. For a spatially-distributed system we

1 write the steady-state equations as

$$\begin{aligned}
2 \quad & \mathcal{D}\Delta u + F(u, \Phi(x)) = 0 && \text{in } \Omega \\
3 \quad & && \\
4 \quad & -\mathcal{D}\frac{\partial u}{\partial n} = B(u, \Phi_B) && \text{on } \partial\Omega
\end{aligned} \tag{2.3}$$

5 where \mathcal{D} is now an $n \times n$ matrix of dimensionless diffusion constants, and B incorporates the fluxes at
6 the boundary. We assume that this has a unique solution and differentiate (2.3) with respect to Φ to
7 obtain

$$\begin{aligned}
8 \quad & \mathcal{D}\Delta u_\Phi + F_u u_\Phi + F_\Phi = 0 && \text{in } \Omega \\
9 \quad & && \\
10 \quad & -\mathcal{D}\frac{\partial u_\Phi}{\partial n} = B_u(u^s, \Phi_B)u_\Phi^s && \text{on } \partial\Omega.
\end{aligned} \tag{2.4}$$

11 If there are q parameters in Φ , then u_Φ is an $n \times q$ matrix.

12 Now suppose that the boundary between cell types is determined by a threshold value of a particular
13 component u_i , or by a functional (a scalar-valued function) of the solution. The latter might for example
14 be the condition that an activator is above a certain level and the inhibitor is below a certain level. As
15 before, let $\mathcal{R}(u)$ denote the response, and define \mathcal{R}^* as the threshold response. Then at a steady state
16 the level set that corresponds to this threshold defines a set in space – a point in 1D, a curve in 2D, or a
17 surface in 3D – on which the response is at the threshold. On one side of this point, curve or surface –
18 depending on the space dimension – the response is above threshold, while on the other side it is below
19 threshold. This level set is defined implicitly by the relation

$$20 \quad \mathcal{R}(u^s(\xi^*, \Phi)) = \mathcal{R}^* \tag{2.5}$$

where ξ^* is the spatial coordinate on the level set. Let p be one of the entries of Φ ; then by differentiating
(2.5) with respect to the chosen parameter we obtain the following relation for the sensitivity

$$\xi_p^* \equiv \frac{\partial \xi}{\partial p}$$

of the threshold position.

$$\langle \mathcal{R}_u, \nabla u \rangle_{\xi_p^*} + \langle \mathcal{R}_u, u_\Phi \Phi_p \rangle = 0$$

21 Here $\langle \cdot, \cdot \rangle$ denotes the Euclidean inner product, and to simplify the formulae, we use subscripts to denote
22 partial derivatives.

23 Therefore, if $\langle \mathcal{R}_u, \nabla u \rangle \neq 0$,

$$24 \quad \xi_p^* = -\frac{\langle \mathcal{R}_u, u_\Phi \Phi_p \rangle}{\langle \mathcal{R}_u, u_\xi \rangle}. \tag{2.6}$$

25 One sees from (2.6) that two components, given by the numerator and the denominator, contribute to
26 the sensitivity, and increasing the latter reduces the sensitivity of the threshold location. If $\langle \mathcal{R}_u, u_\xi \rangle = 0$,
27 then ξ_p^* is indeterminate at this order.

28 When the response is a function of only one species, (2.6) reduces to

$$29 \quad \xi_p^* = -\frac{u_\Phi \Phi_p}{u_\xi}. \tag{2.7}$$

1 and therefore the derivative \mathcal{R}_u cancels, and as a result **for any response function that depends**
 2 **on only one factor or species, the sensitivity ξ_p^* of a threshold location to a parameter p is**
 3 **independent of the sensitivity \mathcal{R}_u of the response functional to the concentration u .**

4 Thus no matter how complicated the internal signal transduction mechanism may be, if the overall
 5 input-response behavior is as shown in Figure (I) of Table 2, *i.e.*, the downstream response to a
 6 morphogen only depends on that morphogen, then the sensitivity of the location of any threshold level
 7 is independent of the sensitivity of the response functional to the morphogen level. This is a very strong
 8 conclusion, but of course the actual location of the threshold does depend on \mathcal{R} .

9 **2.2.1 The single morphogen scheme**

Consider the scalar, steady-state problem analyzed earlier whose solution is given at (1.5). Suppose
 that the response is defined as

$$\mathcal{R}(u) = \frac{u^{n_h}}{1 + u^{n_h}},$$

10 and that the threshold is set at $\mathcal{R}^* \in (0, 1)$. This defines the first Scheme I in Table 2. For simplicity
 11 let us assume that the reaction time T_k is short enough compare to diffusion time T_d so that δ is small.
 12 With this assumption, the boundary at $x = L$ has a negligible effect. Then

$$13 \quad u^* = \left(\frac{\mathcal{R}}{1 - \mathcal{R}} \right)^{\frac{1}{n_h}} \quad (2.8)$$

14 and

$$15 \quad \xi^* = \delta \left(\ln J\delta - \frac{1}{n_h} \ln \frac{\mathcal{R}}{1 - \mathcal{R}} \right). \quad (2.9)$$

16 In particular, if $\mathcal{R}^* = 0.5$, then $u^* = 1$ and

17

$$\xi^* = \delta \ln J\delta, \quad \xi_\delta^* = 1 + \ln(J\delta), \quad \text{and} \quad \xi_J^* = \frac{\delta}{J}.$$

18 Thus ξ_δ^* is one when $T_{rd} = T_i$, and otherwise depends on the relative size of these time scales. It only
 19 vanishes if $\ln(J\delta) = -1$, but then ξ^* lies outside the domain. Therefore one cannot guarantee robust
 20 placement of the boundary location under changes in the ratio of the time scales defined by δ . Since
 21 $\xi_J^* = \delta/J = \sqrt{\mathcal{D}^3 K^2 / (kj^2 L^4)}$, sensitivity with respect to the input flux is decreased by decreasing the
 22 diffusion coefficient or increasing the degradation rate or the input flux. One also sees that in either
 23 case the location of the threshold and its sensitivity with respect to parameters are independent of n_h
 24 for $\mathcal{R}^* = 0.5$, and therefore of the steepness of the response at the chosen threshold. However this is not
 25 true for other choices of the threshold, as (2.9) shows. Calculation of the sensitivities of the location
 26 with respect to the measurable quantities such as the diffusion coefficient or the input flux requires one
 27 additional step.

28 We consider Scheme I as a base case for later comparison with other signaling schemes. For this
 29 purpose we compute the response and the location of the boundary numerically for several thresholds,
 30 and for a range of input fluxes and δ , using the exact solution of the steady-state problem (1.5). It
 31 follows from (1.5) and (2.7) that $(u)_\xi < 0$, $(u)_\delta > 0$, and $(u)_J > 0$, and therefore the boundary
 32 position ξ^* moves rightward as either δ or J are increased, as expected. The base parameters $\delta = 0.1$

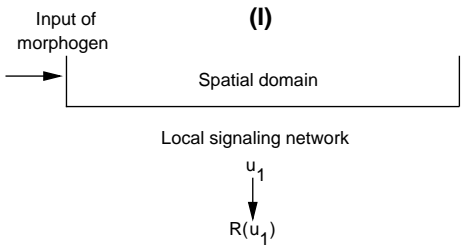
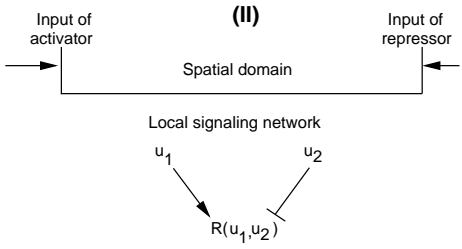
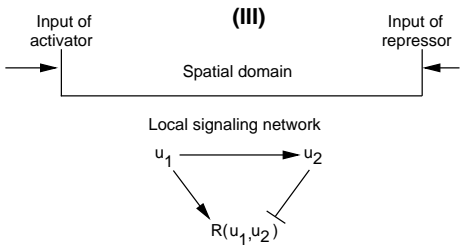
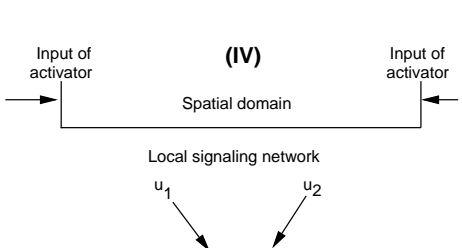
Signaling Scheme	Governing Equations	Response Functional
<p style="text-align: center;">(I)</p> 	$\delta^2 \frac{d^2 u}{d\xi^2} = u \quad \xi \in (0, 1)$ $-\frac{du}{d\xi} = J \quad \xi = 0$ $\frac{du}{d\xi} = 0 \quad \xi = 1,$	$\mathcal{R}(u) = \frac{u^{n_h}}{1 + u^{n_h}}$ $u(\xi) = J\delta \left[\frac{e^{-\xi/\delta} + e^{(\xi-2)/\delta}}{1 - e^{-2/\delta}} \right]$ $\equiv Jh(\delta, \xi)$
<p style="text-align: center;">(II)</p> 	$\delta_1^2 \frac{d^2 u_1}{d\xi^2} = u_1 \quad \delta_2^2 \frac{d^2 u_2}{d\xi^2} = u_2 \quad \xi \in (0, 1)$ $-\frac{du_1}{d\xi} = J_1 \quad \frac{du_2}{d\xi} = 0 \quad \xi = 0$ $\frac{du_1}{d\xi} = 0 \quad \frac{du_2}{d\xi} = J_2 \quad \xi = 1,$	$\mathcal{R}(u) = \frac{u_1^{n_{h1}}}{1 + u_1^{n_{h1}}} \cdot \frac{1}{1 + u_2^{n_{h2}}}$ $u_1(\xi) = J_1 h(\delta_1, \xi)$ $u_2(\xi) = J_2 \delta_2 \left[\frac{e^{(1-\xi)/\delta_2} + e^{(1+\xi)/\delta_2}}{e^{2/\delta_2} - 1} \right]$ $\equiv J_2 z(\delta_2, \xi)$
<p style="text-align: center;">(III)</p> 	$\delta_1^2 \frac{d^2 u_1}{d\xi^2} = u_1 \quad \delta_2^2 \frac{d^2 u_2}{d\xi^2} = -\kappa u_1 + u_2 \quad \xi \in (0, 1)$ $-\frac{du_1}{d\xi} = J_1 \quad \frac{du_2}{d\xi} = 0 \quad \xi = 0$ $\frac{du_1}{d\xi} = 0 \quad \frac{du_2}{d\xi} = J_2 \quad \xi = 1,$	$\mathcal{R}(u) \text{ and } u_1 \text{ are as in Scheme II.}$ $u_2(\xi) = J_2 z(\delta_2, \xi)$ $+ \frac{\kappa J_1 [h(\delta_1, \xi) - h(\delta_2, \xi)]}{1 - (\delta_2/\delta_1)^2} 1_{\{\delta_1 \neq \delta_2\}}$ $+ \frac{\kappa J_1 \delta_1 h_{\delta_1}(\delta_1, \xi)}{2} 1_{\{\delta_1 = \delta_2\}}$
<p style="text-align: center;">(IV)</p> 	<p style="text-align: center;">The governing equations are as in Scheme II.</p>	$\mathcal{R}(u) = \frac{u_1^{n_{h1}}}{1 + u_1^{n_{h1}}} \cdot \frac{u_2^{n_{h2}}}{1 + u_2^{n_{h2}}}$ <p style="text-align: center;">u_1 and u_2 are as in Scheme II.</p>

Table 2: The signaling schemes in the deterministic analysis. The left column gives the signaling scheme, the center column gives the governing equations, and the third column gives the response functional for that signaling scheme. The notation 1_a is equal to 1 if the condition a is true, and zero if it is false.

- 1 corresponds to a half-life $k^{-1} \sim 20$ min, a diffusion coefficient $\mathcal{D} = 1\mu\text{m}^2/\text{sec}$, and a domain length
- 2 of length $L = 100\mu\text{m}$. Using a reference concentration $K = 0.1\mu\text{M}$, the base input flux $j = K\mathcal{D}J/L$
- 3 corresponds to 600 molecules/ $(\mu\text{m}^2 \text{sec})$. The morphogen profile and the response profile for these base
- 4 values and three values of the Hill coefficient are shown in Figure 3 (left), and the response surface as
- 5 a function of δ is shown in Figure 3 (right).

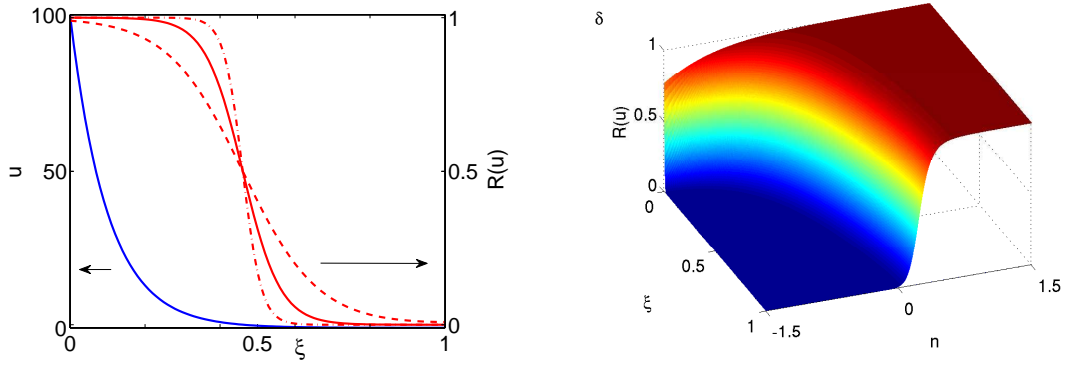


Figure 3: (Left) The morphogen profile (blue) and the response function (red) for Scheme I, using the base parameters $\delta = 0.1$, and $J = 10^3$, and $n_h = 1, 2$ and 4 . (Right) The response surface as a function of δ and ξ , where $\delta = 10^{n-1}$.

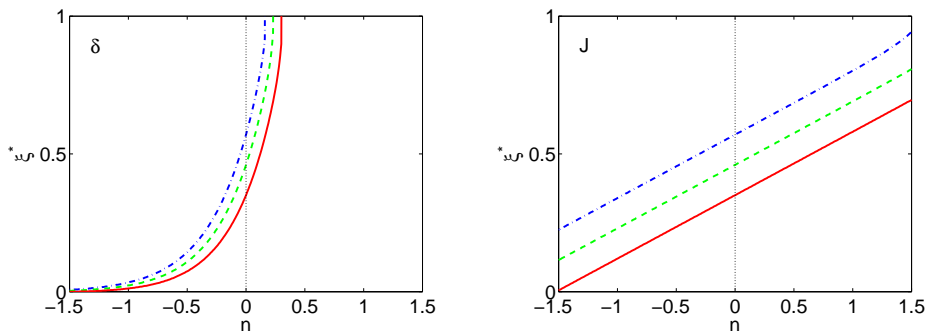


Figure 4: The spatial location of the specified thresholds as a function of δ (left) and J (right) for Scheme I. The parameters are given by $\delta = 10^{n-1}$ (left) and $J = 10^{n+3}$ (right) using the base set. Here and hereafter blue (dash-dot lines), green (dashed lines) and red (solid lines), denote thresholds $\mathcal{R}^* = 0.25, 0.5, 0.75$, respectively.

1 The computed threshold positions as a function of δ and J are shown in Figure 4 for threshold
2 levels of $\mathcal{R}^* = 0.25, 0.5, 0.75$. As δ increases, the effect of diffusion time scale decreases relative to that
3 of reaction. This leads to an increase in the morphogen concentration and the response throughout
4 the domain, and therefore the threshold positions determined by the chosen thresholds move rightward
5 and for sufficiently large δ lie at the boundary (*cf.* Figure 4 (left)). An increase in the dimensionless
6 input flux J has a similar but less dramatic effect – the morphogen concentration increases in direct
7 proportion with J , as seen from (1.5), and thus the threshold location moves further into the domain.
8 In either case we can conclude that boundary placement under Scheme I is not robust to variations in
9 the dimensionless parameters δ or J .

10 For the base parameters and thresholds chosen, an increase in the Hill coefficient has little effect
11 on the robustness, despite the fact that the response is sharpened (*cf.* Figure 3 (left)), because the
12 morphogen gradient is steep for the chosen thresholds in the response. However an increase in n_h has
13 a significant effect at lower thresholds, but the effect of this for a wider parametric range remains to
14 be investigated. Of course other forms of single-morphogen response functions may lead to different
15 conclusions, but would require some biological motivation.

2.2.2 Signaling schemes with independent activation and inhibition

There are numerous other more complex signaling schemes used in pattern formation, several of which are shown in Table 2. The next simplest is one in which a morphogen that initiates activation of gene transcription is produced at one end of the domain, while an inhibitory signal that represses transcription is produced at the other end, as shown in Scheme II of the table. In this scheme there is no upstream interaction between the morphogens, and they exert their effect on the response independently. The bicoid-nanos-hunchback system, in which bicoid activates expression of hunchback whereas nanos represses it [37], is an example of this signaling scheme.

Since the morphogens do not interact, the activating signal, denoted u_1 , is as in the previous example with δ and J replaced by δ_1 and J_1 . Denote by u_2 the dimensionless concentration of the inhibitory morphogen, and suppose that this morphogen is produced at $\xi = 1$. Detailed governing equations for u_1 and u_2 are given in Table 2. The response function is chosen to be

$$\mathcal{R}(u) = \mathcal{F}_1(u_1)\mathcal{F}_2(u_2) = \frac{u_1^{n_{h_1}}}{1 + u_1^{n_{h_1}}} \cdot \frac{1}{1 + u_2^{n_{h_2}}} \quad (2.10)$$

where the n_{h_i} 's represent the respective Hill coefficients. This form arises, for example, when activating and inhibiting transcription factors bind independently to a promoter [38]. We choose the same thresholds as before and let η^* denote the spatial position corresponding to a threshold, *i.e.*, $\mathcal{R}(u(\eta^*)) = \mathcal{R}^*$. In addition, we let ξ^* be the spatial location of the threshold when $u_2 = 0$, in which case the response in Scheme II reduces to that in Scheme I. When $u_2 \neq 0$, $\mathcal{F}_2|_{\xi=\eta^*} < 1$, and it follows from the fact that $\mathcal{F}_1|_{\xi=\xi^*} = \mathcal{F}_1 \cdot \mathcal{F}_2|_{\xi=\eta^*} = \mathcal{R}^*$ and the monotonicity of \mathcal{F}_1 that $\xi^* > \eta^*$. In other words, adding an inhibitor lowers the overall response level and retains a decreasing response gradient with the maximum level at the source location of the activator, as in Scheme I. Therefore, the boundary location determined by the threshold moves toward the source of the activator, as expected.

In Figure 5 we show the effect of changes in the δ_i s when both are equal. When both are small ($n < 0$) the location of the threshold increases with δ_i , as in Figure 4. However, due to the effect of the inhibitor, the threshold location in Figure 5 is generally closer to the activator source than it is in Figure 4. On the other hand, when both exceed the base value $n = 0$ the threshold locations rapidly move toward $\xi = 0$, and for sufficiently large δ_i the thresholds are never reached. This can be understood in terms of the competing processes involved. As the δ_i s are increased, the effect of diffusion relative to degradation increases and the level of both the activator and the inhibitor increases. When both δ_i s are small, the level of both the activator and the inhibitor are low, $\mathcal{F}_1 \ll 1$ and $\mathcal{F}_2 \approx 1$ in (2.10), and the effect of the increased activator on the response is larger than that of the increased inhibitor. As a result, the location of the threshold moves toward the inhibitor source. When $\delta_1 = \delta_2$ is large, the level of both the activator and the inhibitor is larger, $\mathcal{F}_1 \approx 1$ and $\mathcal{F}_2 \ll 1$ in (2.10), and as a result, the effect of the increased inhibitor on the response dominates and the location of the threshold moves toward the activator source. The effect of varying the input fluxes simultaneously is less dramatic – in each case the threshold position first moves outward from $\xi = 0$ and then gradually retreats. Simultaneous variation in the Hill coefficients of activator and inhibitor has little effect on the threshold locations.

The effects are quite different when the δ 's are varied independently, as shown in Figure 6. At fixed δ_2 , increasing δ_1 moves the threshold outward from $\xi = 0$, similar to both the single morphogen and the symmetric activator-inhibitor cases. However, for $n > 0$ the threshold location stabilizes because

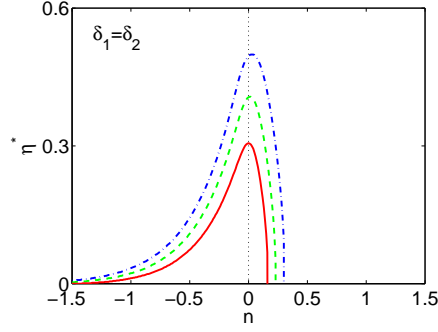


Figure 5: The threshold location as a function of δ for equal δ_i s in Scheme II. Here $J_i = 10^3$ and $n_{h_i} = 1$.

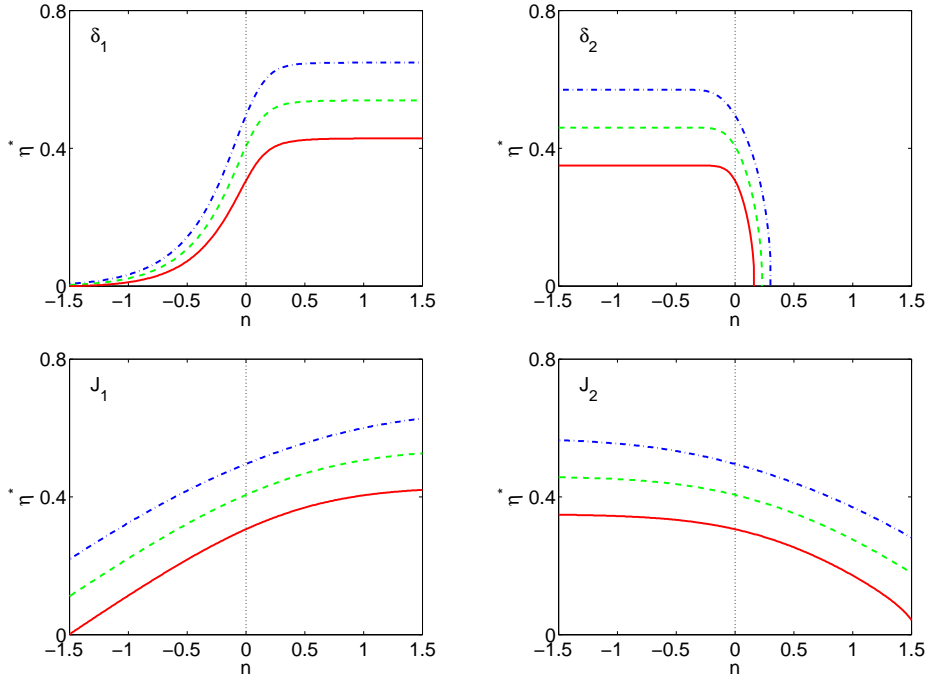


Figure 6: The signaling scheme with asymmetric activator and inhibitor: The parameter that varies is indicated on each panel, $\delta_i = 10^{n-1}$ (top) and $J_i = 10^{n+3}$ (bottom) and the base parameters are $\delta_1 = \delta_2 = 0.1$, $J_1 = J_2 = 10^3$, and $n_{h_i} = 1$.

1 the activation is saturated and the response is determined by the inhibitor, which accounts for the
2 plateau. The transition value of δ_1 for different thresholds is essentially independent of the threshold.
3 Similarly, when δ_2 is sufficiently small the effect of the activator dominates and the threshold location
4 is independent of δ_2 . In fact the results in Figure 5 can be understood as the diagonal slice of a 3D
5 representation of the top panels in Figure 6.

6 The effect of the input fluxes is less pronounced, as seen in Figure 6. The threshold positions are
7 shifted toward $\xi = 0$, since inclusion of the inhibitor lowers the level of response slightly, and for small
8 values of J_1 they increase approximately linearly, as in Figure 4. However the effect of the inhibitor
9 limits the increase as activation saturates, and the cumulative effect is less over the full range. Similarly,
10 the effect of the inhibitor flux is weak at low inputs but stronger at high inputs, and the thresholds
11 are moved significantly leftward toward the activator source due to the lower level of response as we
12 increase J_2 . The Hill coefficients of activator and inhibitor have little effect on the boundary positions

1 determined by the thresholds because the gradients of activator and inhibitor are quite steep.

2 Thus the inclusion of an independently-acting inhibitor can significantly reduce the sensitivity of
 3 threshold locations to variations in the dimensionless parameters δ_i in suitable ranges, and thus lead
 4 to robustness of the placement of the boundary between cell types. The large values of δ_1 needed for
 5 fixed values of the remaining parameters can be achieved by increasing the diffusion coefficient or the
 6 half-life of the activator, and inversely for smaller values of δ_2 . However this signaling scheme does not
 7 lead to precise boundary location in the face of variations in the input fluxes.

8 2.2.3 The incoherent feedforward network

9 The question then arises whether upstream interactions between activator and inhibitor can increase
 10 the robustness. As an example, we add production of the inhibitor catalyzed by the activator, as shown
 11 in Scheme III of Table 2, to the previous network. Since the additional production of the inhibitor
 12 increases its level throughout the domain, the boundary location ζ^* corresponding to the threshold \mathcal{R}^* ,
 13 which is implicitly defined by $\mathcal{R}(u(\zeta^*)) = \mathcal{R}^*$, moves toward the activator source, *i.e.*, $\zeta^* < \eta^*$.

14 The introduction of a catalytic effect of the activator on the inhibitor leads to some different effects
 15 under variation of some parameters. The variation of the threshold with δ_1 shown in Figure 7 is
 16 qualitatively similar to that in the symmetric case shown in Figure 5, although the maxima for lower
 17 thresholds are displaced to larger n . However, the effect of increases in the input flux of activator is
 18 very different. At small values of J_1 the variation of the threshold is similar to that shown in Figure 6,
 19 but for large J_1 the higher level of activator induces more inhibitor and the threshold level sets intersect
 20 $\zeta^* = 0$. Thus, depending on n , one has either a super-threshold region from 0 to an upper value of ζ ,
 21 or an interior super-threshold region, surrounded by sub-threshold regions near each boundary.

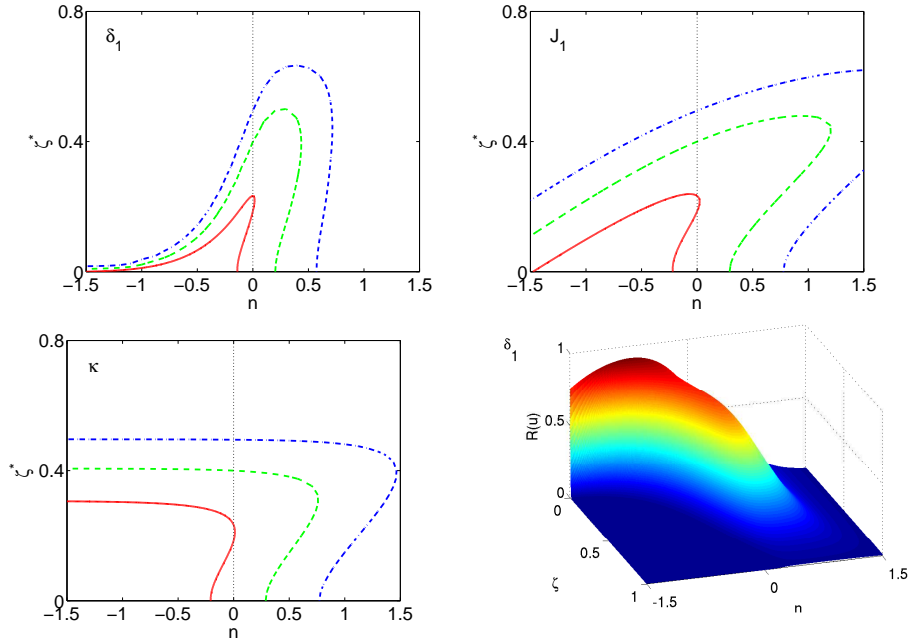


Figure 7: The signaling scheme using activator-catalyzed production of the inhibitor: (top) Both the parameter variations and the base parameters are as before. (bottom left) The variation of the threshold position with the catalytic production rate for $\kappa = 10^{n-2}$ and, (bottom right) the dependence of the response function on δ_1 .

1 The variation of the threshold position with δ_2 and J_2 is less dramatic and similar to that shown
2 in Figure 6, except for a slight decrease of the overall response level. On the other hand, the catalytic
3 parameter also has a significant effect. As shown in Figure 7, for small values of κ ($n < 0$), boundary
4 positions are insensitive as expected, since this reduces to a previous signaling scheme with independent
5 activation and inhibition, but if κ is sufficiently large the inhibitor effect dominates and the threshold
6 eventually retracts to $\zeta = 0$ due to a lower level of response. However, between the low and high values
7 lies a region in which there are threshold crossings, which again leads to an interior region of gene
8 expression.

9 2.2.4 A dual activator signaling scheme

10 In the final example of the deterministic analysis we suppose that both morphogens are activators and
11 thus both enhance the response, as shown in Scheme IV of Table 2. Since activators are produced at both
12 ends and both must be sufficiently large to produce a super-threshold response, one expects activation in
13 a band, the sharpness of which should be determined by the Hill coefficients. The completely symmetric
14 case (equal inputs, equal decay lengths, and equal Hill coefficients) is easiest to analyze, but a parametric
15 study in the case of unequal parameters for the two morphogens reveals some interesting effects. The
16 results for variations in δ_1 and J_1 are shown in Figure 8, and the results for the second pair are similar,
17 relative to $\xi = 1$.

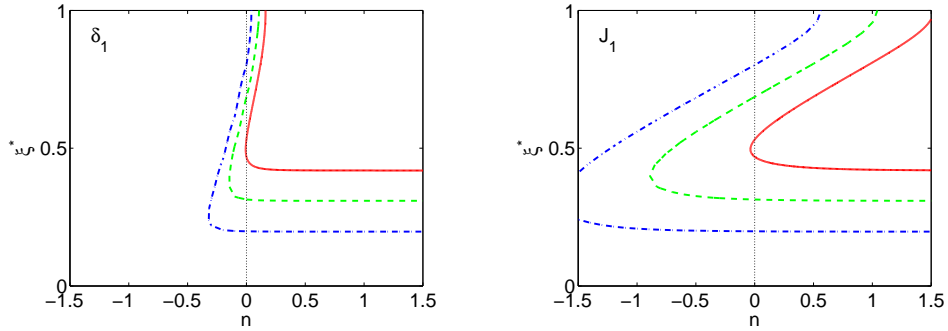


Figure 8: The signaling scheme with two activators: $\delta_1 = 10^{n-1}$ (left) and $J_1 = 10^{n+4}$ (right). The base values of the parameters are $\delta_1 = \delta_2 = 0.1$, $J_1 = J_2 = 10^4$ and $n_{hi} = 1$.

18 In Figure 8, we divide the loci for ξ^* into two parts, the upper, increasing part of the curve, and the
19 lower, flat part of the curve, and denote them by ξ_u^* and ξ_l^* . At $n = 0$ the system is symmetric and the
20 results in Figure 8 reflect this, but as δ_1 is increased the concentration of u_1 increases rapidly pointwise,
21 and the left-most boundary (smallest ξ^*) for $\mathcal{R}^* = 0.25$ stabilizes at $\xi_l^* \approx 0.2$ for $n > \sim -0.25$, and
22 similarly for other thresholds. However, the upper boundary ξ_u^* increases rapidly with δ_1 , and reaches 1
23 for n small and positive, and beyond this value the interval $(\xi_l^*, 1]$ is above threshold and thus is turned
24 ‘on’.

25 The results are qualitatively similar as J_1 is varied. The location of the boundary for the lowest
26 threshold is essentially fixed over the entire range of J_1 shown, whereas the upper boundary increases
27 approximately log-linearly. Thus the location of the lower boundary of the activated region is relatively
28 insensitive for a wide range of both the dimensionless diffusion rate δ_1 and the dimensionless input flux
29 J_1 , more so for the latter than the former, but the upper boundary moves as either parameter is varied,

1 rapidly in the case of δ_1 and more slowly in the case of J_1 .

2 **3 The robustness of threshold positions in stochastic models**

3 **3.1 Static interpretation for simple systems**

4 Stochastic effects can play an important role in gene expression and spatial pattern formation in de-
 5 velopment if key components are present in low copy numbers. For example, gene transcription in
 6 some bacteria involves interactions between 1-3 promoter elements and 10-20 copies of repressor pro-
 7 teins [39], while in DV patterning of *Drosophila* it is known that Dpp signaling increases from a low
 8 basal rate to the maximal rate in the range of $10^{-10}M$ to $10^{-9}M$ [40], and at these concentrations
 9 there are on average fewer than 10 signaling molecules
 10 per nucleus. Since chemical reactions occur in discrete
 11 steps at the molecular level, the processes are inherently
 12 stochastic and the inherent “irreproducibility” in these
 13 dynamics has been demonstrated experimentally for sin-
 14 gle cell gene expression events [41, 42]. However, in gen-
 15 eral, organisms show a remarkable degree of resilience or
 16 robustness in the face of noise, and thus understanding
 17 the dynamics of a system of interacting species and how
 18 noise influences the outcome is important in numerous
 19 contexts.

20 To illustrate the importance of fluctuations due to
 21 small numbers of molecules, consider the French flag
 22 problem discussed earlier. Figure 9 shows one realiza-
 23 tion of a stochastic model of a linear chain of cells in
 24 which the input flux is fixed at the left. The solid line
 25 shows the mean of the distribution, which can be com-
 26 puted directly since the equations are linear [43]. This
 27 curve also represents the steady-state distribution for
 28 the corresponding deterministic system. Since each de-
 29 veloping embryo represents one realization of the stochastic patterning process, the results illustrate the
 30 difficulty in determining the location of the boundaries between cell types in the face of such fluctua-
 31 tions. Clearly fluctuations will be significant, and how the embryos cope with them to pattern reliably
 32 is not understood. Thus it is important to determine how the structure of the signaling scheme, which
 33 involves both the spatial arrangement of morphogen sources and the structure of the signal transduc-
 34 tion network, affects the outcome. Of course, the spatial variation of morphogens adds a new level of
 35 complexity to the problem, and raises the question as to what the role of diffusion is in filtering the
 36 noise. It certainly removes rapidly varying spatial components, and this has the effect of removing high
 37 frequency components in inputs. In this section, we focus on the effect of different types of spatial
 38 signaling schemes on the fluctuations in the boundary location.

39 To eliminate the ‘salt-and-pepper’ effect seen in Figure 9, cells must adopt the right type for their
 40 spatial location with a high probability, and this leads to the criterion defined later for the precision of

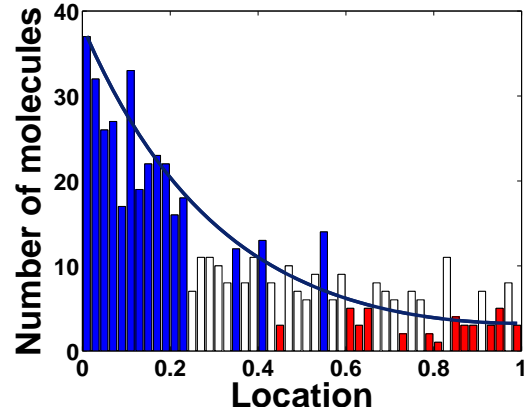


Figure 9: One realization of the French flag model with stochastic dynamics, shown at 100 mins. The system comprises 50 compartments, each $1 \times 0.01 \times 0.01 \text{ mm}^3$, the diffusion coefficient is $1000 \mu\text{m}^2 \text{ min}^{-1}$, the influx from a source at the left end is at a rate $0.1 \text{ nM } \mu\text{m} \text{ min}^{-1}$, and diffusion and degradation occur at a rate of 0.01 min^{-1} . Each compartment has 10 morphogen molecules initially. Color indicates the thresholds: blue – greater than 12, and white – greater than 6 molecules.

1 boundary location. As before, if a functional of the morphogen level in a cell is above a threshold value,
 2 we assume that the cell becomes type I, and otherwise, it becomes type II. The first objective is to
 3 determine how different response functionals couple with gradient formation mechanisms to determine
 4 the probability that the cell adopts one of two types. At the multicellular level we expect that the
 5 domain can be divided into different regions, in some of which the cells have a high probability to be of
 6 type I and in others the cells have a high probability of becoming type II. We define a type I domain as
 7 one in which the cells have a probability greater than 0.5 of being of type I, and we therefore choose as
 8 the boundary between regions of different types the locus on which the probability is approximately 0.5.
 9 As shown below, this criterion can be used to understand how different response functionals affect the
 10 robustness of boundary location. A 1D compartmentalized system with two simple signaling schemes
 11 is used to illustrate the major ideas and conclusions.

12 3.1.1 The single activator scheme

13 We first analyze the stochastic version of Scheme I described in Table 2. Assume that the system is
 14 of length L , that the morphogen is injected at the left end, and that the opposite end is impermeable.
 15 The morphogen undergoes degradation at a rate k throughout the system and diffuses with diffusion
 16 coefficient \mathcal{D} . We discretize the system into ν identical compartments and assume that morphogen
 17 production occurs in the first compartment as a Poisson process of rate s . We denote by N_i the number of
 18 morphogen molecules in the i th compartment, and then the stationary distribution of (N_1, N_2, \dots, N_ν)
 19 is given as

$$20 \quad P(N_1 = n_1, N_2 = n_2, \dots, N_\nu = n_\nu) = \prod_{i=1}^{\nu} e^{-M_i} \cdot \frac{M_i^{n_i}}{n_i!}, \quad (3.1)$$

21 where M_i is the mean number of molecules in the i th compartment at the steady state [43, 44].

22 We first calculate $M = (M_1, M_2, \dots, M_\nu)$ to determine the mean, and then we define the response
 23 functional and use the stationary distribution to study the boundary location. The mean concentrations
 24 $M = (M_1, M_2, \dots, M_\nu)$ satisfy the difference equation

$$25 \quad \delta^2 \nu^2 \Delta_\nu M - I_\nu M + S_\nu = 0, \quad (3.2)$$

where $\delta = \sqrt{\mathcal{D}/(kL^2)}$ is as defined previously, I_ν is the $\nu \times \nu$ identity matrix, $S_\nu = (s/k, 0, \dots, 0)'$ and
 Δ_ν is the $\nu \times \nu$ matrix

$$\Delta_\nu = \begin{pmatrix} -2 & 2 & & & & \\ & 1 & -2 & 1 & & \\ & & 1 & -2 & 1 & \\ & & & \ddots & \ddots & \\ & & & & 1 & -2 & 1 \\ & & & & & 2 & -2 \end{pmatrix}.$$

26 If we discretize the 1D domain in (1.4) into ν intervals using centered differences, and let c_i be the
 27 morphogen concentration in the i th interval, then

$$28 \quad \delta^2 \nu^2 \Delta_\nu c - I_\nu c + J_\nu = 0, \quad (3.3)$$

where $J_\nu = (2j\nu/(kL), \dots, 0)^T$. Therefore, for consistency between the descriptions we must have

$$M = c \cdot \mathcal{N}_A \cdot V \quad \text{and} \quad s = \frac{2j\nu}{L} \cdot \mathcal{N}_A \cdot V,$$

1 where \mathcal{N}_A is Avagadro's number and V is the volume of a compartment.

The solution of (3.2) is then given by

$$M = \frac{s}{k} \sum_{j=1}^{\nu} \frac{\mathcal{P}_j}{1 - \alpha_j \delta^2},$$

2 where α_j is the j th eigenvalue of Δ_ν and \mathcal{P}_j is the corresponding projection of Δ_ν . There are no
3 nilpotents in this representation because Δ_ν is semisimple, but the eigenvalues and eigenvectors must
4 be computed numerically.

5 **3.1.2 The stationary distribution of the cell types**

6 As in the deterministic analysis, we scale the signal level so that the half-maximal response in the Hill
7 function is at $u = 1$. Thus if there are n_i morphogen molecules in the i th compartment, the response is

$$8 \quad \mathcal{R}_i = \frac{u_i^{n_i}}{1 + u_i^{n_i}}, \quad (3.4)$$

9 where $u_i = n_i/\Omega$ and $\Omega \equiv \mathcal{N}_A \cdot K \cdot V$. Let \mathcal{R}^* be the threshold value and let u^* be the corresponding
10 concentration, which is given by (2.8). Then the probability that the i th compartment is of type I is
11 the marginal cumulative distribution

$$12 \quad \begin{aligned} P_i &\equiv Pr(N_i \geq \lceil u^* \cdot \Omega \rceil) \\ &= \sum_{n_i \geq \lceil u^* \cdot \Omega \rceil} e^{-M_i} \times \frac{M_i^{n_i}}{n_i!}, \end{aligned} \quad (3.5)$$

14 where $\lceil u^* \cdot \Omega \rceil$ is the smallest integer greater than or equal to $u^* \cdot \Omega$. This is obtained by summing over
15 all but the i^{th} factor in (3.1) and using the fact that the sums are one.

16 Since P_i increases with M_i , and the latter is monotone decreasing with i , we define the boundary as
17 the smallest i such that $P_i < 0.5$. To define the cell type, we define the discrete random variable Θ_i as

$$18 \quad \Theta_i = \begin{cases} 1 & \text{if } N_i \geq \lceil u^* \cdot \Omega \rceil, \\ 0 & \text{otherwise.} \end{cases}$$

Thus Θ_i is a Bernoulli random variable and

$$P(\Theta_i = 1) = P_i, \quad P(\Theta_i = 0) = 1 - P_i, \quad E(\Theta_i) = P_i, \quad Var(\Theta_i) = P_i(1 - P_i).$$

19 Therefore, $E(\Theta_i)$ is the expectation that the i th compartment is of type I and $Var(\Theta_i)$ measures the
20 spread in the types of the i th compartment around the expectation. The variance is largest for $P_i = 0.5$,
21 as a reasonable definition of the boundary between cell types requires.

22 To illustrate how $E(\Theta_i)$ and $Var(\Theta_i)$ depend on the threshold, which determines u^* , we show $E(\Theta_i)$
23 and $Var(\Theta_i)$ as a function of the compartment number in the 1D system in Figure 10. In the left panel

1 one sees that $E(\Theta_i)$ is close to one on the left-most part of the system and drops rapidly to zero toward
2 the right hand boundary of the system for both $\mathcal{R}^* = 0.5$ and 0.75 . Using these thresholds the system
3 can be divided into two regions: in region (I) most of the compartments are of type I, and in region
4 (II) most of the compartments are of type II. Correspondingly, $Var(\Theta_i)$ is almost zero in the interior of
5 the two regions, but larger at the boundary between them, as expected. $E(\Theta_i)$ varies more slowly and
6 the variance has broader support when the threshold is set at $\mathcal{R}^* = 0.25$, as is to be expected, since the
7 threshold lies in a region where the morphogen distribution varies more slowly.

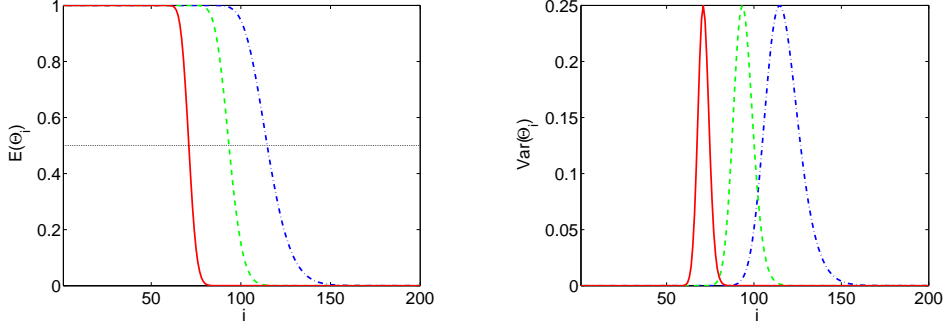


Figure 10: The mean and variance of the random variable that determines the cell types in the stochastic version of Scheme I. The x-axis is the number of the compartment. In this figure and in Figure 11 we use the base values $\nu = 200$, $L = 400\mu m$, $V = 2\mu m \times 0.3\mu m \times 0.3\mu m$, $\mathcal{D} = 1\mu m^2/s$, $K = 0.2\mu M$, $k = 6.25 \times 10^{-4}/s$, $\delta = \sqrt{\mathcal{D}/(kL^2)} = 0.1$ and $J = jL/(K\mathcal{D}) = 10^3$ in the calculation. As in the deterministic analysis, red solid lines correspond to $\mathcal{R}^* = 0.75$, dashed green lines correspond to $\mathcal{R}^* = 0.5$ and dash-dot blue lines correspond to $\mathcal{R}^* = 0.25$.

8 Thus we can conclude that setting a higher threshold response in the single-activator system produces
9 a better localization of the boundary between cell types by increasing the steepness of the P_i distribution
10 and thereby decreasing the width of the variance distribution. This conclusion will hold for any number
11 of thresholds, as long as they have the same functional form of the response at each threshold. However
12 there are known examples in which the functional form itself changes depending on the morphogen level,
13 *e. g.*, by activating at one level and inhibiting at another, and the analysis has to be extended for such
14 systems.

15 Since u^* is given by (2.8) one sees that if $\mathcal{R}^* < 0.5$, increasing the Hill coefficient n_h in the response
16 function increases u^* , which moves the boundary location towards the activator source and attenuates
17 the fluctuations in the determination of cell types. Conversely, if $\mathcal{R}^* > 0.5$, increasing n amplifies the
18 fluctuations in the determination of cell types. Therefore, as stated in the deterministic section, the
19 effect of increasing the Hill coefficient on the precision of the determination of cells types depends on
20 whether \mathcal{R}^* is larger or less than 0.5. Furthermore, since $u^* > \mathcal{R}^*$, the boundary location defined by
21 using the Hill function is closer to the activator source than that defined by using the morphogen level
22 directly, and therefore passing the fluctuating morphogen concentration through the nonlinear response
23 filters the noise and reduces the spread of the variance in the determination of cell types.

24 To illustrate that the general conclusions concerning the dependence of the threshold location on pa-
25 rameters reached for the deterministic system also apply here, we show in Figure 11 how the boundary
26 location determined by $P_i = 0.5$ changes as the dimensionless diffusion coefficient δ and the dimen-
27 sionless flux J are changed. For comparison with the deterministic model, we scale the compartment
28 number from zero to one. Figure 11 shows that the dependence of the boundary location on J and δ is

- 1 qualitatively the same as that in the deterministic model, but a more precise comparison will be made
 2 elsewhere.

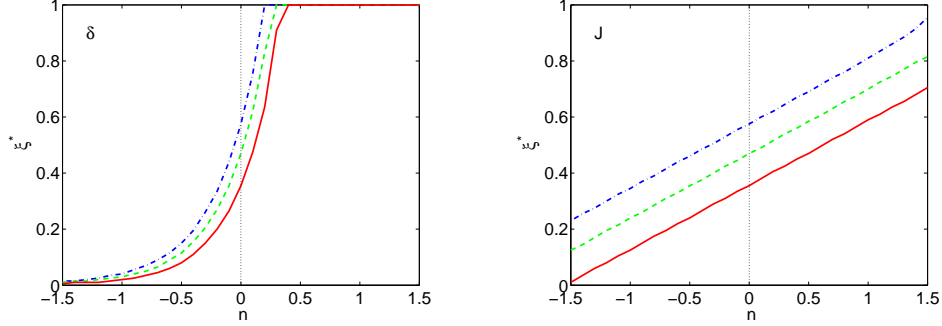


Figure 11: The variation of the boundary locations as the flux and dimensionless diffusion coefficient are varied in the stochastic version of Scheme I. The y-axis is the compartment number normalized by 200 and the x-axis indicates the variation of the parameters. In the left panel $\delta = 10^{n-1}$, and in the right panel $J = 10^{3+n}$.

3 Since \mathcal{R}^* is a deterministic function of the morphogen level u , the consistency between the stochastic
 4 predictions (Figure 11) and the deterministic predictions (Figure 4) indicates that the deterministic
 5 model is sufficient to study the sensitivity of the boundary location to parameters if the downstream
 6 network is deterministic, or if it is stochastic but relaxes rapidly. As in the deterministic system,
 7 adjusting the threshold level can reduce the fluctuations in the determination of cell types, and using
 8 Hill functions to define the downstream response rather than the morphogen level can also be used to
 9 reduce the variation in the boundary location. Hill functions are widely used in gene control networks
 10 to capture the fast reactions between DNA and transcription factors, but a more detailed multi-scale
 11 stochastic analysis is needed to justify treating this step deterministically [45], especially as there are
 12 only a few copies of most genes.

13 3.1.3 The activator-inhibitor signaling scheme

Next we consider the independent activator-inhibitor network (Scheme II) in one space dimension,
 and as before, we discretize the system into ν identical compartments. The activating morphogen is
 produced in the first compartment with rate s_1 and the inhibiting morphogen is produced in the ν th
 compartment with rate s_2 . Parameters such as decay constants and diffusion rates are as defined in
 section 2.2.2. Let $N_{1,i}$ and $N_{2,i}$ denote the random numbers of the activator morphogen molecules and
 the inhibitor morphogen molecules in the i th compartment respectively. The stationary distribution
 of $N_{1,i}$ and $N_{2,i}$ can be derived as in the single-activator system. If there are $n_{1,i}$ activator molecules
 and $n_{2,i}$ inhibitor molecules in the i th compartment, the response of the i th compartment is defined as
 follows.

$$\mathcal{R}_i(n_{1,i}, n_{2,i}) = \frac{u_{1,i}^{n_{h_1}}}{1 + u_{1,i}^{n_{h_1}}} \cdot \frac{1}{1 + u_{2,i}^{n_{h_2}}}$$

where

$$u_{1,i} = \frac{n_{1,i}}{\Omega_1} \quad \text{and} \quad u_{2,i} = \frac{n_{2,i}}{\Omega_2},$$

1 $\Omega_i \equiv \mathcal{N}_A \cdot K_i \cdot V$ and K_1, K_2, n_{h_1} and n_{h_2} are constants. Letting \mathcal{R}^* be the threshold value, the
 2 probability of the i th compartment being of type I is

$$\begin{aligned}
 3 \quad P_i &= \sum_{\mathcal{R}_i(n_{1,i}, n_{2,i}) \geq \mathcal{R}^*} P(N_{1,i} = n_{1,i}, N_{2,i} = n_{2,i}) \\
 4 \quad &= \sum_{\mathcal{R}_i(n_{1,i}, n_{2,i}) \geq \mathcal{R}^*} P(N_{1,i} = n_{1,i})P(N_{2,i} = n_{2,i}).
 \end{aligned}$$

5 In this system the threshold depends on both species and therefore we define the Bernoulli variable that
 6 determines the cell type as

$$7 \quad \Theta_i = \begin{cases} 1 & \text{if } \mathcal{R}_i(N_{1,i}, N_{2,i}) \geq \mathcal{R}^*, \\ 0 & \text{otherwise,} \end{cases}$$

8 and we show $E(\Theta_i)$ and $Var(\Theta_i)$ for the 1D system in Figure 12. As in to Figure 10, the 1D system can
 9 be divided into two regions. In the type I region, $E(\Theta_i)$ is close to one and $Var(\Theta_i)$ is close to zero, while
 10 in the type II region both $E(\Theta_i)$ and $Var(\Theta_i)$ are close to zero. The boundary defined by the threshold
 $P_i = 0.5$ lies between these two regions. However in contrast with the single-activator scheme, in Figure

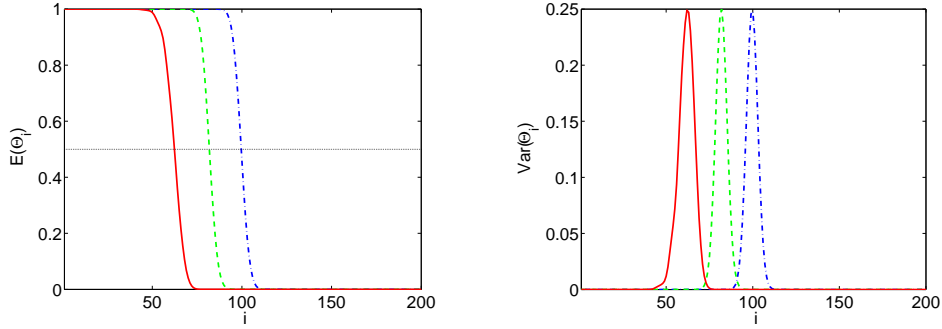


Figure 12: The fluctuations in the determination of cell types in the activator-inhibitor signaling system. The x-axis is the compartment number. Here and in Figure 13, the base parameters are $\nu = 200$, $L = 400\mu m$, $V = 2\mu m \times 0.3\mu m \times 0.3\mu m$, $\mathcal{D}_1 = \mathcal{D}_2 = 1\mu m^2/s$, $K_1 = K_2 = 0.2\mu M$, $k_1 = k_2 = 6.25 \times 10^{-4}/s$, $\delta_1 = \sqrt{\mathcal{D}_1/(k_1 L^2)} = 0.1$, $\delta_2 = \sqrt{\mathcal{D}_2/(k_2 L^2)} = 0.1$, $J_1 = j_1 L/(K_1 \mathcal{D}_1) = 10^3$, $J_2 = j_2 L/(K_2 \mathcal{D}_2) = 10^3$, $n_{1,h} = 1$ and $n_{2,h} = 1$.

11
 12 the distribution of the variance is much more concentrated for the two lowest thresholds, whereas
 13 in Figure 10, $Var(\Theta_i)$ has broader support for $\mathcal{R}^* = 0.25$. The deterministic analysis of the single-
 14 activator system predicts that the sensitivity of the location of the threshold is inversely proportional to
 15 the gradient of the morphogen (*cf.* (2.7), and therefore one expects a broader distribution of the variance
 16 and larger fluctuations in the position for lower thresholds. In the activator-inhibitor system the effect
 17 of the inhibitor is strongest where the activator concentration is lowest, and this sharpens the spatial
 18 distribution of the variance significantly. Thus the addition of the inhibitor increases the precision with
 19 which the boundary between cell types is determined.

20 In Figure 13, we show how the boundary location changes as the dimensionless flux and diffusion
 21 coefficients change. To be consistent with the deterministic model, we scale the compartment number
 22 from zero to one. Just as in the single-activator case (*cf.* Figure 11), the dependence of the boundary
 23 location on J_1, J_2, δ_1 and δ_2 is qualitatively the same as that in the deterministic model. The addition of

- 1 one inhibitor sharpens the signal gradient and reduces the fluctuations in the determination of cell types.
- 2 Therefore, in addition to the downstream network, the upstream signaling scheme is very important for
- 3 signal precision.

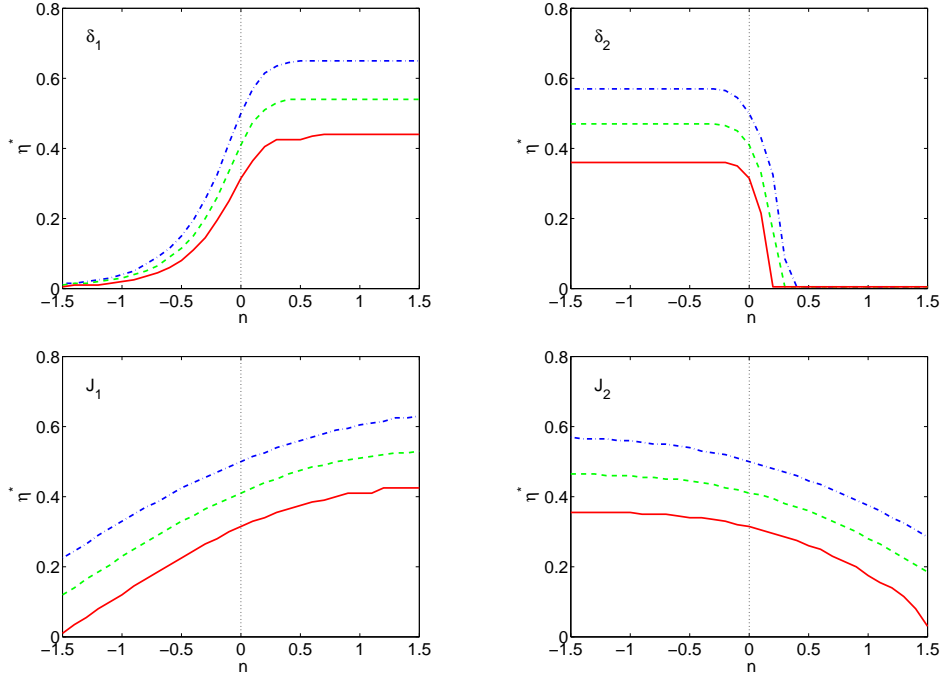


Figure 13: The variations of the boundary locations as the flux and dimensionless diffusion coefficient are varied in the activator-inhibitor signaling system. The y-axis is the scaled compartment number and the x-axis indicates how we vary the parameters.

4 3.2 A model for activation of receptor production by morphogen-bound receptors

5 The final example is a 1D system with morphogen produced at one end and a feedback loop catalyzing
6 the production of receptors throughout the domain (*cf.* Figure 14 (left)). This model is used to under-
7 stand how the feedback loop couples with other reaction and diffusion processes to affect the precision
8 of the boundary location. It provides a simplified description of systems such as the hedgehog-patched
9 system illustrated in Figure 1, which arises in pattern formation in the *Drosophila* wing disc and in the
10 vertebrate limb. Denote by M , R , MR and P the morphogen, receptor, morphogen-bound receptor
11 and downstream product protein, respectively, in the kinetic scheme shown in Figure 14 (right).
12 Here $f(p)$ is a function of the concentration of the protein P that controls the production of the receptor
13 R . Let m , r , mr and p denote the concentrations of M , R , MR and P at position x at time t , and
14 assume that morphogen M diffuses throughout the system with diffusion coefficient \mathcal{D}_m . The governing
15 deterministic equations of the system are as follows:

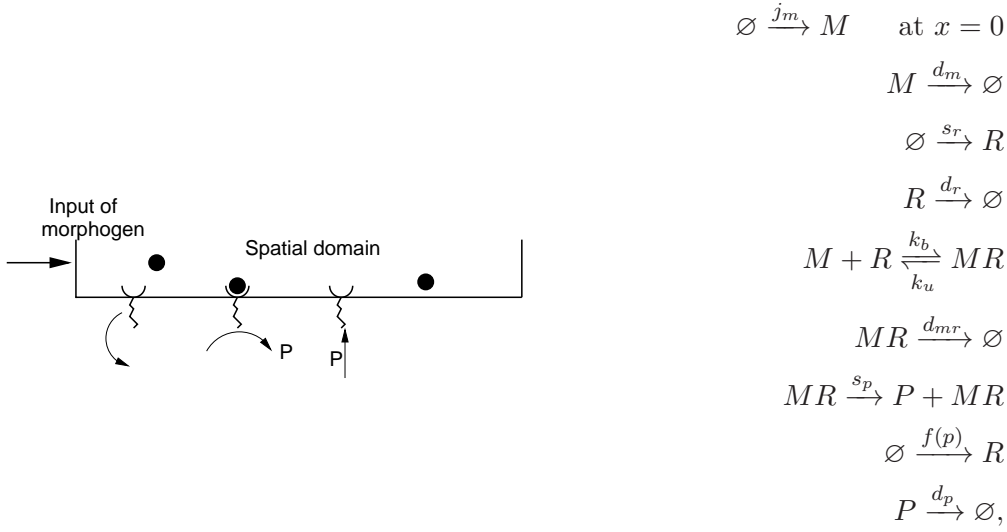


Figure 14: (Left) The signaling scheme with positive feedback. (Right) The kinetic mechanism.

$$\begin{aligned}
1 & \quad \frac{\partial m}{\partial t} = \mathcal{D}_m \Delta m - d_m m - k_b m \cdot r + k_u m r \\
2 & \quad \frac{\partial r}{\partial t} = s_r - d_r \cdot r - k_b m \cdot r + k_u m r + f(p) \\
3 & \quad \frac{\partial m r}{\partial t} = k_b m \cdot r - k_u m r - d_{m r} m r \\
4 & \quad \frac{\partial p}{\partial t} = s_p m r - d_p p \\
5 & \quad -\mathcal{D}_m \left. \frac{\partial m}{\partial x} \right|_{x=0} = j_m, \quad \mathcal{D}_m \left. \frac{\partial m}{\partial x} \right|_{x=L} = 0,
\end{aligned} \tag{3.6}$$

where

$$f(p) = C_p \cdot \frac{p^{n_h}}{K^{n_h} + p^{n_h}}.$$

6 In the following simulations we always begin with a zero initial concentration for all species.

7 Since the system is nonlinear, we cannot determine the morphogen profiles analytically, even in a
8 stationary state, and we use the Gillespie stochastic simulation algorithm [46] to study the distribution
9 of the boundary location numerically. Here we consider a line of 25 compartments, where each com-
10 partment is a rectangular domain of dimension $0.3\mu\text{m} \times 0.3\mu\text{m} \times 3\mu\text{m}$. Morphogen M is produced in
11 the first compartment, and the base values of parameters are as follows.

$$\begin{aligned}
12 & \quad j_m = 9.9 \times 10^{-3} \mu\text{M}/s, \quad s_r = 6.2 \times 10^{-5} \mu\text{M}/s, \quad s_p = 1/s \\
13 & \quad d_m = 0, \quad d_r = 6.25 \times 10^{-4}/s, \quad d_{m r} = 6.9 \times 10^{-2}/s, \quad d_p = 6.25 \times 10^{-3}/s \\
14 & \quad \mathcal{D}_m = 1\mu\text{m}^2/s, \quad k_b = 7.15 \times 10^{-2}/\mu\text{M}/s, \quad k_u = 6.25 \times 10^{-4}/s, \\
15 & \quad C_p = 1.1 \times 10^{-3} \mu\text{M}/s, \quad K = 4.8 \times 10^{-2} \mu\text{M}, \quad n_h = 3.
\end{aligned}$$

16 We use the level of the protein P as a surrogate for the response and therefore define the cell type by
17 the concentration of P – if it is above K the compartment is defined as type I; otherwise it is defined to

1 be type II. We use the compartment of type II that is closest to the source of M to define the boundary.
 2 Figure 15 shows the mean concentration profile of P , and from this see that for the base values of the
 3 parameters the boundary is at the 7th cell.

4
 5 Simulations in which one parameter is varied and the
 6 remainder fixed show how the distribution of the bound-
 7 ary locations is affected by changes in the parameters.
 8 Figures 16-(a), (b) and (c) show the effect of changes in
 9 the parameters \mathcal{D}_m , k_b , and d_m , which control diffusion,
 10 binding, and decay, respectively, of free morphogen. In-
 11 creasing \mathcal{D}_m or decreasing k_b and d_m flattens the profile
 12 of M and thereby shifts the mean outward and increases
 13 the spread of the variance in the distribution of bound-
 14 ary locations. The shift of the mean is most pronounced
 15 for \mathcal{D}_m , whereas the increase in the spread of the vari-
 16 ance is most pronounced for changes in the on-rate k_b .

17 The latter stems from the fact that reducing k_b increases the spread of the morphogen and decreases
 18 the production of P . However, decreasing d_m does not affect the boundary location significantly, as
 19 can be seen in Figure 16-(c), which indicates that the degradation rate of the free morphogen has little
 20 effect for the range considered.

21 Figure 16-(d) shows that changing the degradation rate of the receptors has a much larger effect
 22 on the boundary location. For large d_r ($n = 1$ in that panel) the location is widely distributed, but as
 23 d_r decreases the threshold location centers at around 15 for $n = 2$ and then decreases steadily as d_r is
 24 decreased further. This can be understood by noting that as d_r is decreased, the level of the receptors
 25 and the protein P increase, which thereby increases the feedback, and as a result the boundary between
 26 cell types moves toward the source of the morphogen.

27 Decreasing the degradation or internalization rate d_{mr} of bound receptors will lead to an increase
 28 in the level of bound receptors MR , and hence increase the level of P , which moves the location of the
 29 boundary away from the morphogen source, as one sees in Figure 16-(e). When d_{mr} is greater or equal
 30 to $6.9/s$ ($n=1$ in that panel) the signal density in all compartments is below the threshold value. When
 31 d_{mr} is less than that ($n \geq 2$) the signal density near the morphogen source is above the threshold value
 32 and the boundary location falls into the first few compartments near the source. The distribution of
 33 locations is relatively narrow for this parameter.

34 Figure 16-(f), (g) and (h) show how the parameters in the Hill function affect the distribution of
 35 the boundary location. One finds that when $K \leq 4.8 \times 10^{-2} \mu M$, changing K and n does not change
 36 the profiles of P much (results not shown). Therefore, the distribution of the boundary location does
 37 not change much in Figure 16-(f) and (g). When $K = 4.8 \mu M$ ($n=1$ in panel (f)) saturation in $f(p)$ is
 38 never reached and the gradient in the profile of P is shallow and the distribution of boundary locations
 39 is broader. Similarly, as C_p decreases from $1.1 \times 10^{-2} \mu M/s$ to $1.1 \times 10^{-4} \mu M/s$, the profile of P becomes
 40 flatter and the boundary location moves away from the morphogen source and becomes more broadly
 41 distributed. However, when C_p is less than $1.1 \times 10^{-4} \mu M/s$, the level of receptors is small, the profile
 42 of P is low and almost flat, and the distribution of locations is very broad.

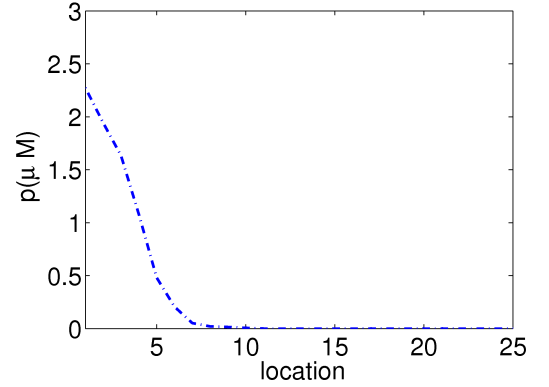


Figure 15: The mean concentration of P for the base values of all parameters.

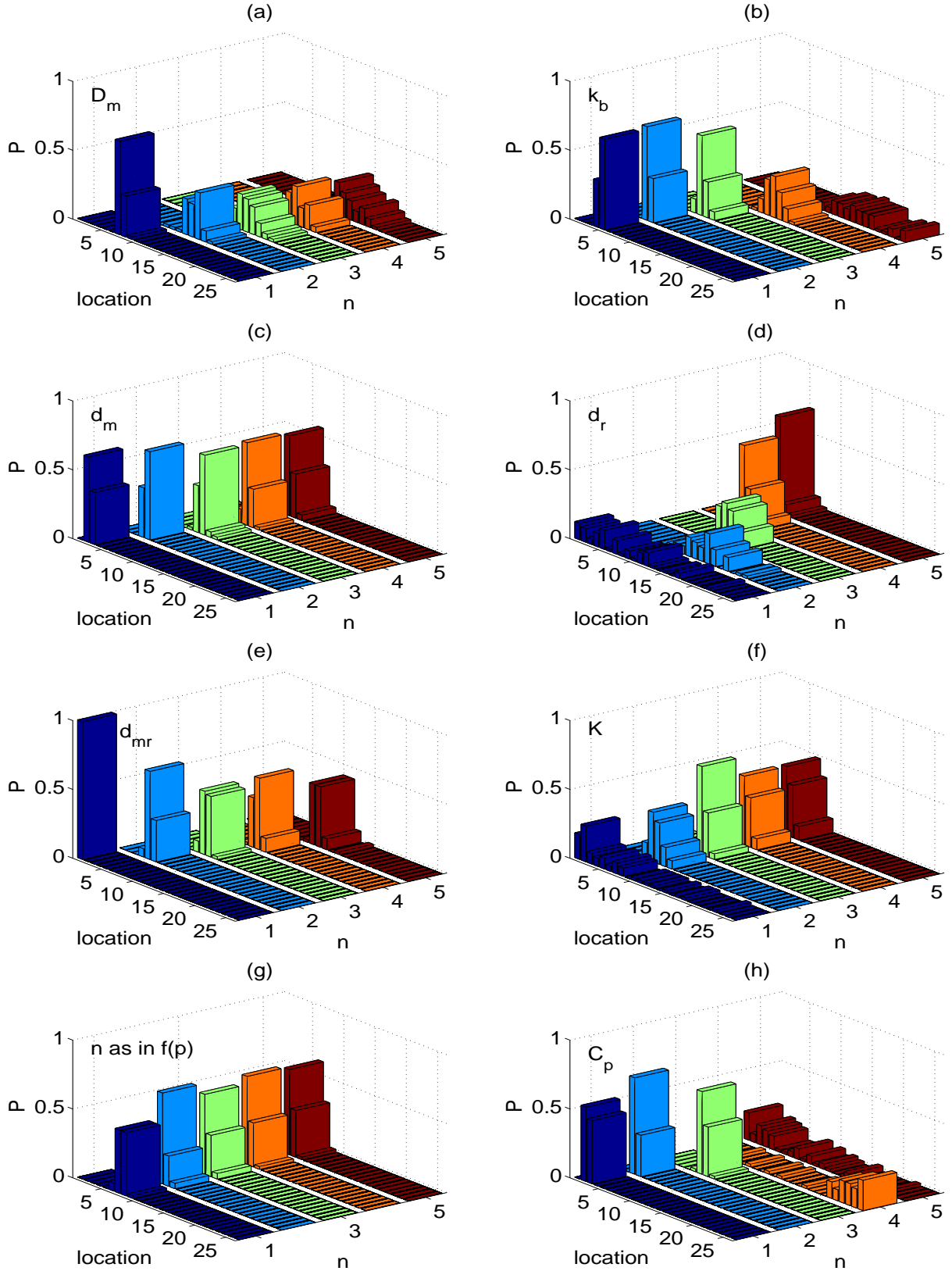


Figure 16: The distribution of the threshold locations with varying parameters. In (a) $D_m = (10n - 9)\mu m^2/s$; in (b) $k_b = 7.15 \times 10^{1-n}/\mu M/s$; in (c) $d_m = 6.25 \times 10^{-n}/s$; in (d), $d_r = 6.25 \times 10^{-n}/s$; in (e), $d_{mr} = 6.9 \times 10^{1-n}/s$; in (f), $K = 4.8 \times 10^{1-n}\mu M$; in (g), n is the Hill coefficient in $f(p)$; and in (h), $C_p = 1.1 \times 10^{-n}\mu M/s$.

1 In conclusion, the effect of \mathcal{D}_m , d_m and d_{mr} on signaling is similar to their effect in the linear systems,
2 while the effect of d_r on the boundary location can be biphasic. Moreover, the effect of C_p can be much
3 larger than those of K and n , since C_p determines the strength of the feedback loop.

4 4 Conclusions

5 Despite the fact that many have analyzed the effect of noise on the location of a specified threshold
6 morphogen level [47, 48, 49, 50], how developing systems reliably partition a tissue into distinct cell types
7 is still poorly understood. Here we have shown, both by a deterministic and a stochastic analysis, how
8 the number and location of morphogen sources and the downstream interpretation of the morphogen
9 levels affect the precision with which the boundary between cell types can be determined.

10 In Section 1.2 we showed how level sets propagate in reaction diffusion systems and suggested how
11 dual morphogen systems can lead to advance and retreat of threshold levels, depending on how rapidly
12 different morphogens relax to a quasi-steady state. This only occurs when several morphogens are
13 involved, and may shed light on the observed variation in the positions of gap gene expression. This
14 analysis may also provide further insight into the role of positive feedback in localizing gene expression
15 in other systems [11].

16 While cells exposed to morphogens sample their environment continuously, the establishment of
17 morphogen distributions is often sufficiently rapid compared to the time scale of gene expression to
18 justify a static analysis, as was done in Section 2.1. Our objective throughout was to understand how
19 the placement of the morphogen source(s) and the type of interpretation function used as the response
20 affect the location of specified level sets of the response. This analysis was only done in 1D, but the
21 general approach can be used in 2D or 3D as well. This approach requires both the determination of the
22 level sets of the morphogen(s) and those of the response, and in the deterministic example studied here
23 there was no feedback from the downstream response to the signal transduction steps. This simplified
24 the analysis, but the inclusion of feedback is important in many cases, and one example was studied in
25 the stochastic analysis in Section 3.2.

26 We found that the sensitivity of the response, as measured by the Hill coefficient, has little effect on
27 the robustness of threshold location when thresholds are set at levels at which the morphogen gradient is
28 large, as predicted by the analysis of the single-activator system. However, in results not shown we find
29 that when the threshold is set at a level for which the morphogen profile varies slowly, the sensitivity
30 of the response can have a large effect. Probably both mechanisms are used in different systems, but
31 there is little quantitative data available on this. Using four simple examples with an activator and
32 an inhibitor, we have shown how the boundary positions change as we vary parameter values. The
33 least robust to changes in the dimensionless diffusion coefficient(s) and the dimensionless input flux(es)
34 is the single activator system. Simply adding an inhibitor produced on the boundary opposite to the
35 activator production can significantly improve the robustness with respect to the δ_i s, but the effect on
36 the sensitivity with respect to input fluxes is less dramatic. The example using an incoherent feedforward
37 network showed a very interesting effect, in that for certain parameters the activated (above threshold)
38 region lay in an interval interior to the domain (*cf.* Figure 7). This can be understood by realizing that
39 if the activator also catalyzes production of the inhibitor, then the inhibitor will become large in regions
40 of high activator and diminish the response.

1 In the stochastic framework we developed a new and novel method for defining the boundary between
 2 cell types by appropriately quantizing the probability of exceeding a specified threshold in the number
 3 of a downstream molecule, and we have shown that the predictions are consistent with those of a
 4 deterministic model. We also analyzed a positive feedback system and showed that the model predicts
 5 robustness with respect to certain parameters such as the diffusion coefficient (when small enough), the
 6 degradation rate of the ligand-free receptor, and several parameters in the feedback function. Since
 7 the stochastic analysis also predicts the variance in the underlying distribution, one can predict the
 8 variations in location of the boundary between cell types. One important conclusion not obtained
 9 from the deterministic analysis is that the shape of the profile of $E(\Theta_i)$ is critical for the precision of
 10 determining the boundary between cell types, since $E(\Theta_i)$ determines $Var(\Theta_i)$ in our approach.

11 As an example of the stochastic effects in boundary determination, segment determination in
 12 *Drosophila*, which is governed by the expression of the pair-rule and segment polarity genes, is a quasi-
 13 one-dimensional process, in that it varies in the anterior-posterior direction. The network governing
 14 expression of the segment polarity genes is reasonably well understood and predicts robust boundary
 placement given the correct initial conditions [51, 52]. Nonetheless, the location of the boundary of

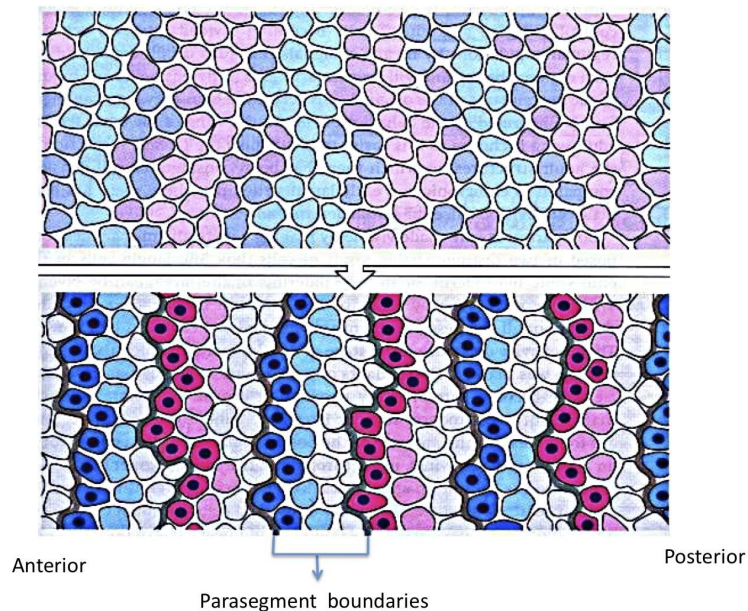


Figure 17: Boundary formation due to expression of pair-rule genes in *Drosophila* at an early (top) and later (bottom) stage. Blue: *fushi tarazu*, pink: *even-skipped* and purple dots *engrailed*. From [53], with permission.

15 parasegments in adjacent lines of cells can vary at an earlier stage in which the pair-rule genes are
 16 expressed (Figure 17), but detailed statistics of this variation have not been reported. The approach
 17 developed here could be used to predict the variations from the known network of pair-rule genes and
 18 those predictions compared with reported observations. Of course the one- or two-step processes studied
 19 here (reading of either the morphogen directly or passing the signal through an interpretation function)
 20 will not be correct for these variations in boundary position, and further downstream mechanisms are
 21 needed. A second step may refine the initial location by interactions between adjacent rows of cells,
 22 either via cell sorting based on the expression of surface markers, or by subsequent changes in gene
 23 expression triggered by feedback circuits.
 24

1 **Acknowledgments** This publication was based on work supported in part by NIH Grant # GM29123
2 and in part by Award # KUK-C1-013-04, made by King Abdullah University of Science and Technology
3 (KAUST), and by the Mathematical Biosciences Institute.

4 **References**

- 5 [1] Turing, A. M. 1952. *Phil. Trans. R. Soc. Lond. B* **237**, 37–72.
- 6 [2] Lander, A. D., Nie, Q., and Wan, F. Y. 2002. *Dev Cell* **2**(6), 785–96.
- 7 [3] Kerszberg, M. and Wolpert, L. 1998. *J. Theor. Biol.* **191**, 103–114.
- 8 [4] Child, C. M. *Patterns and Problems of Development*. University of Chicago press, Chicago, 1941.
- 9 [5] Oppenheimer, J. M. *Essays in the History of Embryology and Biology*. MIT Press, 1967.
- 10 [6] Gierer, A. and Meinhardt, H. 1972. *Biological Cybernetics* **12**(1), 30–39.
- 11 [7] Meinhardt, H. *Models of Biological Pattern Formation*. Academic Press, London, 1982.
- 12 [8] Othmer, H. G. In *Dynamics of Synergetic Systems*, Haken, H., editor, 1980.
- 13 [9] Cross, M. C. and Hohenberg, P. C. 1993. *Rev. Mod. Phys.* **65**(3), 851–1112.
- 14 [10] Wolpert, L. 1969. *J. Theor. Biol.* **25**, 1–47.
- 15 [11] Umulis, D. M., Serpe, M., O’Connor, M. B., and Othmer, H. G. August 1 (2006). *Proc Natl Acad*
16 *Sci U S A* **103**(31), 11613–8.
- 17 [12] Othmer, H. G., Painter, K., Umulis, D., and Xue, C. 2009. *Math. Mod. Nat. Phenom.* **4**, 3–79.
- 18 [13] Kicheva, A., Pantazis, P., Bollenbach, T., Kalaidzidis, Y., Bittig, T., Julicher, F., and Gonzalez-
19 Gaitan, M. January (2007). *Science* **315**(5811), 521–525.
- 20 [14] Freeman, M. 2000. *Nature* **408**, 313–319.
- 21 [15] Alon, U. *An introduction to systems biology: design principles of biological circuits*, volume 10.
22 CRC Press, 2007.
- 23 [16] Dillon, R. and Othmer, H. G. 1999. *J. Theor. Biol.* **197**(3), 295–330.
- 24 [17] Little, S. C., Tkačik, G., Kneeland, T. B., Wieschaus, E. F., and Gregor, T. 2011. *PLoS biology*
25 **9**(3), e1000596.
- 26 [18] Gregor, T., McGregor, A. P., and Wieschaus, E. F. 2008. *Developmental Biology* **316**(2), 350–8.
- 27 [19] Bergmann, S., Sandler, O., Sberro, H., Shnider, S., Schejter, E., BZ, B. Z. S., and Barkai, N. 2007.
28 *PLoS Biol.* **5**(2), e46.
- 29 [20] Umulis, D. M. 2009. *J. Roy. Soc. Interface* **6**, 1179–1191.

- 1 [21] Grimm, O., Coppey, M., and Wieschaus, E. 2010. *Development* **137**(14), 2253.
- 2 [22] Spirov, A., Fahmy, K., Schneider, M., Frei, E., Noll, M., and Baumgartner, S. February (2009).
3 *Development* **136**, 605–614.
- 4 [23] Foe, V. E., Odell, G., and Edgar, B. 1993. *The development of Drosophila melanogaster* **1**, 149–300.
- 5 [24] Entchev, E. V., Schwabedissen, A., and Gonzalez-Gaitan, M. 2000. *Cell* **103**(6), 981–91.
- 6 [25] Raftery, L. A. and Sutherland, D. J. 2003. *Trends Genet* **19**.
- 7 [26] Wang, Y. C. and Ferguson, E. L. 2005. *Nature* **434**(7030), 229–34.
- 8 [27] Kutejova, E., Briscoe, J., and Kicheva, A. 2009. *Current opinion in genetics & development* **19**(4),
9 315–322.
- 10 [28] Fife, P. C. *Mathematical Aspects of Reacting and Diffusing Systems, Lecture Notes in Biomathe-*
11 *matics*, volume 28. Springer-Verlag, 1979.
- 12 [29] Dillon, R., Gadgil, C., and Othmer, H. G. 2003. *Proc. Natl. Acad. Sci. (USA)* **100**(18), 10152–7.
- 13 [30] Nahmad, M. and Stathopoulos, A. 2009. *PLoS Biology* **7**(9), e1000202.
- 14 [31] Jaeger, J., Surkova, S., Blagov, M., Janssens, H., Kosman, D., Kozlov, K. N., Myasnikova, E.,
15 Vanario-Alonso, C. E., Samsonova, M., Sharp, D. H., and Reinitz, J. 2004. *Nature* **430**(6997),
16 368–71.
- 17 [32] Othmer, H. G. and Pate, E. F. 1980. *Proc. Nat. Acad. Sciences* **77**, 4180–4184.
- 18 [33] Umulis, D. and Othmer, H. G. In preparation, 2012.
- 19 [34] Sontag, E. D. 2003. *Systems & Control Letters* **50**, 119–126.
- 20 [35] Arnold, V. I. and Levi, M. *Geometrical methods in the theory of ordinary differential equations*,
21 volume 250. Springer, 1988.
- 22 [36] Niswander, L., Jeffrey, S., Martin, G. R., and Tickle, C. 1994. *Nature* **371**, 609–612.
- 23 [37] Simpson-Brose, M., Treisman, J., and Desplan, C. September (1994). *Cell* **78**(5), 855–865.
- 24 [38] Tyson, J. J. and Othmer, H. G. 1978. *Progress in Theor. Biol.* **5**, 1–62.
- 25 [39] Kuthan, H. 2001. *Prog Biophys Mol Biol* **75**(1-2), 1–17.
- 26 [40] Shimmi, O. and O’Connor, M. B. 2003. *Development* **130**(19), 4673–4682.
- 27 [41] Spudich, J. L. and Koshland, D. E. 1976. *Nature* **262**, 467–471.
- 28 [42] Levsky, J. M. and Singer, R. H. January (2003). *Trends Cell Biol* **13**(1), 4–6.
- 29 [43] Gadgil, C., Lee, C. H., and Othmer, H. G. 2005. *Bull. Math. Biol.* **67**, 901–946.

- 1 [44] Anderson, D. F., Craciun, G., and Kurtz, T. G. 2010. *Bulletin of mathematical biology* **72**(8),
2 1947–1970.
- 3 [45] Lee, C. H. and Othmer, H. G. In preparation, 2012.
- 4 [46] Gillespie, D. T. 1976. *Journal of Computational Physics* **22**, 403–434.
- 5 [47] Aegerter-Wilmsen, T., Aegerter, C. M., and Bisseling, T. 2005. *J Theor Biol* **234**(1), 13–9.
- 6 [48] Gregor, T., Tank, D. W., Wieschaus, E. F., and Bialek, W. July (2007). *Cell* **130**(1), 153–164.
- 7 [49] He, F., Saunders, T. E., Wen, Y., Cheung, D., Jiao, R., ten Wolde, P. R., Howard, M., and Ma, J.
8 2010. *Biophysical journal* **99**(3), 697–707.
- 9 [50] de Lachapelle, A. M. and Bergmann, S. 2010. *Molecular systems biology* **6**(1), e1001111.
- 10 [51] von Dassow, G., Meir, E., Munro, E. M., and Odell, G. M. 2000. *Nature* **406**(6792), 188–92.
- 11 [52] Albert, R. and Othmer, H. G. 2003. *J. Theor. Biol.* **223**, 1–18.
- 12 [53] Wolpert, L., Beddington, R., Jessel, T., Lawrence, P., Meyerowitz, E., and Smith, J. *Principles of*
13 *Development*. Oxford University Press, 2002.